

THESIS FOR THE DEGREE OF MASTER OF SCIENCE IN COMMUNICATION ENGINEERING

# Uplink Resource Scheduling in Dynamic OFDMA Systems

Farshad Naghibi



**CHALMERS**

Report no. EX069/2008  
Communication Systems  
*Department of Signals and Systems*  
CHALMERS UNIVERSITY OF TECHNOLOGY  
Göteborg, Sweden, 2008



# UPLINK RESOURCE SCHEDULING IN DYNAMIC OFDMA SYSTEMS

FARSHAD NAGHIBI



Thesis performed at:  
Telecommunication Networks Group (TKN),  
Technische Universität Berlin.  
August 2008.

Advisors: Mathias Bohge, Prof. Adam Wolisz (Telecommunication Networks Group)  
Examiner: Prof. Thomas Eriksson (Chalmers University of Technology)

Uplink Resource Scheduling in Dynamic OFDMA Systems

Copyright © 2008 Farshad Naghibi except where otherwise stated. All rights reserved.

Master's Thesis EX069/2008

Communication Systems  
Department of Signals and Systems  
Chalmers University of Technology  
SE-412 96 Göteborg  
Sweden

Telephone +46 - (0)31 - 772 1000

Typeset in L<sup>A</sup>T<sub>E</sub>X2e  
Berlin, Germany 2008

# Abstract

Orthogonal Frequency Division Multiple Access (OFDMA) is among the promising candidates for future generation of wireless communications, due to its robustness to multipath fading, high spectral efficiency as well as its flexibility in resource allocation. In recent years, it has been shown that applying dynamic mechanisms to the downlink of the OFDMA systems, provides a significant increase in the throughput performance.

A major challenge in realizing the uplink transmission in OFDMA systems lies in synchronizing the participating entities. This is mainly due to the fact that in the uplink, each OFDM symbol is formed by the contribution of multiple users. Therefore, OFDMA uplink is more affected by users' timing misalignments. These timing offsets result in loss of subcarrier orthogonality and, thus, lead to multiple access interference (MAI). The usual approach to mitigate MAI in the uplink, is to use relatively long cyclic prefixes as time-domain guard intervals. In this thesis, the use of short time-domain guard intervals in combination with frequency-domain guard bands to protect against MAI, is investigated.

The use of guard bands is studied in two major subcarrier assignment methods: static block assignment and dynamic assignment. In the case of dynamic assignment, two optimization approaches, i.e. raw-rate maximization and max-min capacity optimization, are considered. The formulation of these optimization problems for the uplink, result in non-linear integer programs (IP). Therefore, to solve the optimization problems with linear program solvers, a linear optimization problem is developed that-in combination with a complementary algorithm-can reach a sub-optimal solution.

The results show that using guard bands in a static way, leads to improvements in SINR, but to a loss in transmission capacity, as the SINR gains are not large enough to cover the loss that stems from turning data subcarriers into guard bands. However, using guard bands along with dynamic subcarrier allocation improves the performance according to the respective optimization goal. It is shown that incorporating guard bands in the raw-rate maximization approach yields a higher overall cell capacity, and in the max-min optimization approach yields a valuable increase in the worst user capacity.



# Acknowledgments

This work would have not been possible without the support of many people. First of all, I wish to express my deepest gratitude to my advisor at Telecommunication Networks Group (TKN), Mathias Bohge, for his helpful advices, suggestions and all the discussions we have had throughout the thesis, as well as for his careful review of the thesis report. I would also like to thank him and his wife, Frauke, for their support and all the fun outside the work. I am grateful to Prof. Adam Wolisz for giving me the opportunity to carry out this thesis at his group, and for his valuable insights and guidelines during the course of this work.

I would like to thank Prof. Thomas Eriksson, my examiner at Chalmers University of Technology, for reviewing and evaluating my thesis. Thanks to Nima Seifi, also at Chalmers, for his guidelines and comments on the thesis report.

I am indebted to Prof. James Gross who is now with UMIC Research Center at RWTH Aachen University, for introducing me to such an interesting field, for our great discussions in the early stages of this thesis and for all his support and understanding throughout some of my difficulties in this period. My special thanks also goes to my friends and colleagues at TKN; Marcus Sonnemann, Hyung-Taek Lim, Oscar Puñal (with UMIC Research Center now) and Azzurra La Torre for their help during my time in Berlin, for the coffees, lunches and all the great time we have had together. Moreover, I wish to thank my dear friends, Serveh, Sepehr and Setareh who are always there for me.

Above all, thanks to my lovely family, my parents Hossein and Fariba, my sister Sepideh and my brother Farhad, for their all-time support, patience and encouragement. This thesis is dedicated to them as a token of my gratitude.

FARSHAD NAGHIBI  
Berlin, August 2008



# Contents

<b>Abstract</b>	<b>i</b>
<b>Acknowledgments</b>	<b>iii</b>
<b>Contents</b>	<b>v</b>
<b>List of Figures</b>	<b>vii</b>
<b>List of Tables</b>	<b>ix</b>
<b>List of Abbreviations</b>	<b>xii</b>
<b>1 Introduction</b>	<b>1</b>
1.1 Background . . . . .	1
1.2 Thesis Scope . . . . .	3
1.3 Thesis Outline . . . . .	3
<b>2 Fundamental Concepts</b>	<b>5</b>
2.1 OFDM . . . . .	5
2.1.1 OFDM principles . . . . .	5
2.1.2 OFDM transceiver . . . . .	6
2.1.3 Cyclic prefix . . . . .	8
2.2 OFDMA . . . . .	9
2.3 Resource allocation in OFDMA systems . . . . .	10
2.3.1 Loading algorithms . . . . .	10
2.3.2 Dynamic subcarrier assignments . . . . .	12
<b>3 Related Work and Thesis Approach</b>	<b>13</b>
3.1 Related work on the OFDMA uplink . . . . .	13
3.1.1 Synchronization techniques and guard bands . . . . .	13
3.1.2 Dynamic OFDMA systems . . . . .	14
3.2 Thesis approach . . . . .	16
<b>4 System Model</b>	<b>19</b>
4.1 Wireless channel . . . . .	19
4.2 Transmitter . . . . .	19
4.3 Receiver . . . . .	21

---

4.4	Performance metrics . . . . .	24
4.4.1	SINR . . . . .	24
4.4.2	User capacity . . . . .	24
4.5	Multiple access interference . . . . .	25
4.5.1	MAI mathematical derivation . . . . .	27
<b>5</b>	<b>The Use of Frequency Domain Guard Bands</b>	<b>35</b>
5.1	Guard bands' impact on SINR performance . . . . .	35
5.2	Guard bands' impact on capacity performance . . . . .	38
<b>6</b>	<b>Optimization Approaches</b>	<b>41</b>
6.1	Optimization problem formulation . . . . .	41
6.1.1	Raw-rate maximization . . . . .	42
6.1.2	Max-min capacity optimization . . . . .	43
6.2	Sub-optimal approaches . . . . .	44
<b>7</b>	<b>Performance Evaluation</b>	<b>49</b>
7.1	Methodology . . . . .	49
7.2	Simulation scenario . . . . .	49
7.3	Results . . . . .	50
7.3.1	Raw-rate maximization . . . . .	50
7.3.2	Max-min optimization . . . . .	52
<b>8</b>	<b>Conclusions</b>	<b>57</b>
8.1	Future work . . . . .	58
	<b>Bibliography</b>	<b>59</b>

# List of Figures

1.1	Worldwide growth of mobile and fixed subscribers. . . . .	2
2.1	OFDM signal spectra. . . . .	6
2.2	Saving of bandwidth with OFDM. . . . .	7
2.3	A simple OFDM transceiver. . . . .	8
2.4	Cyclic prefix. . . . .	9
2.5	Channel variations in time, frequency and space. . . . .	10
2.6	Symbol error probability vs. SNR for different QAM types. . . . .	11
4.1	Block diagram of an OFDMA transmitter for uplink. . . . .	20
4.2	Different subchannel assignment methods. . . . .	21
4.3	Block diagram of an OFDMA receiver for uplink. . . . .	22
5.1	The impact of MAI on the average SINR per subchannel. . . . .	37
5.2	The impact of frequency-domain guard bands (GB) on SINR. . . . .	37
5.3	The impact of guard bands on the average capacity per user. . . . .	39
6.1	MAI power as a function of frequency distance. . . . .	46
7.1	Average capacity per user in the raw-rate maximization approach. . . . .	53
7.2	Average capacity per user in the max-min optimization approach. . . . .	55



# List of Tables

- 5.1 Impact of MAI on system capacity. . . . . 38
- 5.2 Impact of guard bands on the system capacity. . . . . 38
  
- 7.1 Simulation scenario, system and channel parameters. . . . . 51
- 7.2 Average cell capacity in raw-rate maximization approach. . . . . 53
- 7.3 Capacity in max-min optimization approach. . . . . 54



# List of Abbreviations

<b>3GPP</b>	Third Generation Partnership Project
<b>ADSL</b>	Asymmetric Digital Subscriber Line
<b>AWGN</b>	Additive White Gaussian Noise
<b>BER</b>	Bit Error Rate
<b>BPSK</b>	Binary Phase Shift Keying
<b>CDMA</b>	Code Division Multiple Access
<b>CFO</b>	Carrier Frequency Offset
<b>CSI</b>	Channel State Information
<b>DAB</b>	Digital Audio Broadcasting
<b>DFT</b>	Discrete Fourier Transform
<b>DVB</b>	Digital Video Broadcasting
<b>FDMA</b>	Frequency Division Multiple Access
<b>FFT</b>	Fast Fourier Transform
<b>ICI</b>	Inter Channel Interference
<b>IDFT</b>	Inverse Discrete Fourier Transform
<b>IEEE</b>	Institute of Electrical and Electronics Engineers
<b>IFFT</b>	Inverse Fast Fourier Transform
<b>IP</b>	Integer Programming
<b>ISI</b>	Inter Symbol Interference
<b>LP</b>	Linear Programming
<b>LTE</b>	Long Term Evolution
<b>MAI</b>	Multiple Access Interference
<b>OFDM</b>	Orthogonal Frequency Division Multiplexing
<b>OFDMA</b>	Orthogonal Frequency Division Multiple Access
<b>PSK</b>	Phase Shift Keying

<b>QPSK</b>	Quadrature Phase Shift Keying
<b>QAM</b>	Quadrature Amplitude Modulation
<b>SER</b>	Symbol Error Rate
<b>SINR</b>	Signal-to-Interference-plus-Noise Ratio
<b>SIR</b>	Signal-to-Interference Ratio
<b>SNR</b>	Signal-to-Noise Ratio
<b>TDMA</b>	Time Division Multiple Access
<b>UMTS</b>	Universal Mobile Telecommunication System
<b>WiMAX</b>	Worldwide Interoperability for Microwave Access
<b>WLAN</b>	Wireless Local Area Network

# Chapter 1

## Introduction

### 1.1 Background

Existing Third-generation (3G) wireless communication systems such as Universal Mobile Telecommunications Systems (UMTS) for wide areas, and Wireless Local Area Networks (WLAN) for local areas, can deliver a maximum data rate of 7.2 Mbps with wide areas of coverage and 54 Mbps with small areas of coverage [1]. However, considering the increase in the number of mobile subscribers in the recent and future years (Figure 1.1) and their expectations for mobile services, brings out the demand for future generation of wireless communication systems to provide much higher data rates than the current systems.

In order to meet the needs for higher data rates, the modulation and multiple access schemes must be chosen in such a way that they provide the system with more flexibility, higher spectral efficiency and more robustness against the impairments of wireless channels. In this regard, one of the most promising candidate technologies which has attracted many attentions in the recent years is Orthogonal Frequency Division Multiplexing (OFDM) [3].

Although the concept of OFDM is not new and can be traced back to the 1950s, its application was very limited due to implementation complexities. In 1971, Weinstein and Ebert [4] suggested an implementation based on Discrete Fourier Transform (DFT) which reduced the complexity to a high degree. Later on, due to the progress in implementation technologies and introduction of Fast Fourier Transform (FFT), OFDM became more popular and used in practice. Since 1990, various systems and standards including Asymmetric Digital Subscriber Lines (ADSL) [5], Digital Audio/Video Broadcasting (DAB/DVB) [6, 7] and wireless LANs [8], adopt OFDM. It has also been proposed for the next generation of mobile communication systems (e.g. Mobile WiMAX [9] and 3GPP LTE [10]).

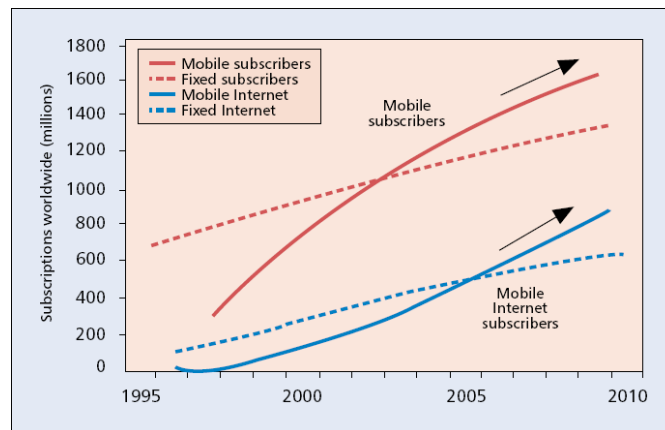


**Figure 1.1:** Worldwide growth of mobile and fixed subscribers [2].

Basically, OFDM converts a high rate data stream into a number of parallel low rate sub-streams and transmits them simultaneously over orthogonal narrow-band subcarriers. Since the symbol duration, which is required for each low rate sub-stream is relatively long, it is inherently more robust against inter symbol interference (ISI). In addition, by adding a guard interval, which usually is a cyclic prefix of the OFDM symbol, the complete elimination of ISI is possible.

There are several ways in which OFDM can be used both as a modulation scheme and also as a multiple access scheme. One way is to combine OFDM with Code Division Multiple Access (CDMA), known as Multi Carrier (MC)-CDMA in which signal is first spread with a spreading code in frequency domain and then sent over the subcarriers. The other technique, called Orthogonal Frequency Division Multiple Access (OFDMA), involves splitting the available subcarriers between different users which is similar to the ordinary Frequency Division Multiple Access (FDMA) except that OFDMA does not require the large guard bands to separate the users. In addition OFDMA can incorporate Time Division Multiple Access (TDMA) for users to access the system in certain time slots [11].

In an OFDMA system, resource allocation refers to allocating subcarriers or a group of subcarriers (chunk or subchannel) to different users and determining the power level and modulation type for the allocated subcarriers. In recent years, a significant gain has been shown to be achievable by applying *dynamic* resource allocation mechanisms to the downlink of OFDM-based multi-user wireless systems. Generally these gains are achieved by exploiting the channel variations for different subcarriers in time, frequency and space.

The base station assigns different set of subcarriers to different users based on the channel state information (CSI) of each subcarrier, to maximize the system performance measure (e.g. minimum throughput of the cell). This mechanism is

called *dynamic subcarrier* allocation. It can also be accompanied by *dynamic power* allocation [12].

In order to achieve similar gains, we would like to adopt the same mechanisms to the uplink of the respective systems. However, moving from downlink to uplink is not straightforward, as in the uplink direction, one OFDM symbol is generated by many different users and then sent to the base station. Consequently, this process might involve problems such as frequency and timing offsets, as well as additional information exchange and signalling overhead. Hence, it is very unlikely that the exact well-known mechanisms can be used in the uplink. Instead, they have to be modified to suit the uplink specific requirements. Especially, because of the missing ideal time synchronization between the terminals in the uplink, subcarriers that are assigned to different terminals cannot be guaranteed to be orthogonal, thus, guard zones (unused parts of the frequency band) might need to be introduced to reduce the interference among the participating entities.

## 1.2 Thesis Scope

This thesis investigates the problem of resource allocation in the uplink of an OFDMA system with the focus on the possible timing misalignment between different users, wherein, the utilization of guard zones to mitigate the impact of these timing offsets is explored. Two main parameters of guard zones are considered, the width and the number of required guard zones. Both parameters have an impact on the available resources for the actual user data transmission: the more and wider guard zones are necessary, the less resources can be used for user data delivery. Finding the optimal trade off between the individuality in subcarrier assignments and the number of necessary guard zones in order to maximize the system throughput or the worst user's throughput is the final objective of this thesis.

## 1.3 Thesis Outline

The rest of the thesis is organized as follows:

In Chapter 2, the basic principles of OFDM as well as OFDMA, along with the related concepts of dynamic resource allocation in such systems are presented. Afterwards, an overview of the existing schemes regarding dynamic resource allocation and synchronization, in the uplink of an OFDMA system is provided in Chapter 3. The model for the system under study is given in Chapter 4. This chapter also includes the MAI model and its detailed mathematical analysis.

In Chapter 5, the usage of frequency-domain guard bands and its impact on the system performance are investigated. The optimization approaches for the uplink of an OFDMA system, including the guard band placement strategies are studied in Chapter 6. Simulation methodology and results along with their analysis are discussed in Chapter 7. Finally in Chapter 8, conclusions are drawn from the results and possible challenges for future work are proposed.

# Chapter 2

## Fundamental Concepts

In this chapter, the essential basic information on OFDM and OFDMA schemes are provided. Thereafter the concept of *dynamic* resource allocation in such systems are described.

### 2.1 OFDM

#### 2.1.1 OFDM principles

Orthogonal Frequency Division Multiplexing is a multi-carrier transmission scheme. The basic idea of OFDM is to divide a high rate data stream into  $N$  low rate sub-streams and send them in parallel over  $N$  subcarriers [11]. In contrast to the conventional multi-carrier schemes, which split the available bandwidth into non-overlapping subcarriers separated by guard bands to prevent inter-carrier interference (ICI), OFDM scheme allows for subcarriers to overlap and still prevents ICI. This is achieved by making subcarriers orthogonal to each other. The orthogonality of subcarriers is resulting from the fact that each subcarrier has an integer number of cycles over an OFDM symbol duration. This ensures that each subcarrier has a null value at the other subcarriers' center frequency. Figure 2.1 shows an example of OFDM signal spectra.

Using orthogonal subcarriers, makes the OFDM systems more spectrally efficient compared to the conventional systems. Figure 2.2 shows the saving of bandwidth with OFDM compared to a conventional multi-carrier scheme with the same subcarrier bandwidth.

The parallel transmission feature of OFDM helps the system to mitigate the effect of multipath delay spread. Since the symbol duration, which is required for

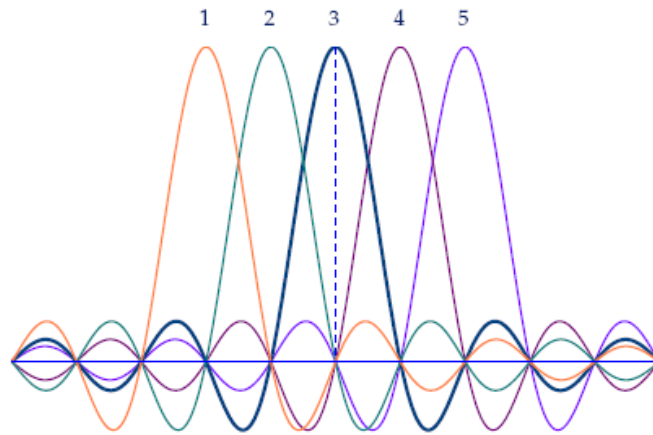


**Figure 2.1:** OFDM signal spectra: each subcarrier has a null value at the other subcarriers' center frequency.

transmitting each low rate sub-stream is relatively long, the OFDM system is more robust to delay spread and consequently ISI is reduced. Furthermore, by using an additional guard interval (cyclic prefix - see Section 2.1.3), at the beginning of each OFDM symbol, ISI can almost be avoided completely.

### 2.1.2 OFDM transceiver

At the OFDM transmitter, the data stream is first split into blocks of  $N$  symbols. Then, the symbols of each block are modulated over the  $N$  subcarriers. The number of bits per symbol is determined by the modulation scheme, which is chosen for each subcarrier. Common modulation schemes include different variations of *Phase Shift Keying (PSK)* and *Quadrature Amplitude Modulation (QAM)*. An OFDM symbol consists of a sum of these modulated subcarriers. Let  $x_n$  be the modulated symbol on subcarrier  $n$  and  $T$  the OFDM symbol duration, then the equivalent complex baseband notation of an OFDM signal starting at  $t = t_s$  can be written as [11]:

$$s(t) = \sum_{i=-\frac{N}{2}}^{\frac{N}{2}-1} x_{i+\frac{N}{2}} \exp\left(j2\pi\frac{i}{T}(t-t_s)\right), \quad t_s \leq t \leq t_s + T \quad (2.1)$$

$$s(t) = 0, \quad t < t_s \wedge t > t_s + T$$

Equation (2.1) is in fact, the real part of the inverse Fourier transform of  $N$

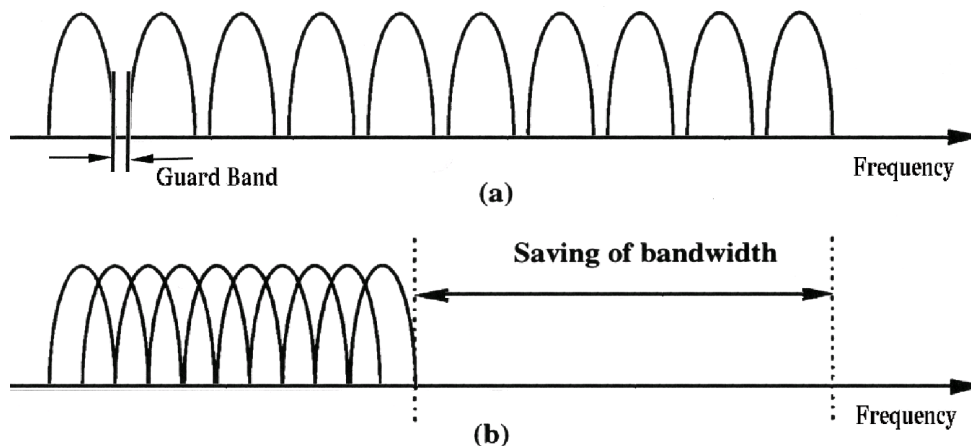


**Figure 2.2:** Saving of bandwidth with OFDM [11]: (a) Conventional multi-carrier scheme and (b) OFDM scheme.

modulated symbols, which is equivalent to Inverse Discrete Fourier Transform (IDFT) in discrete time-domain (as shown in (2.2)) [13]. Note that in the discrete form the time  $t$  is replaced by the sample number  $n$ .

$$s(n) = \sum_{i=0}^{N-1} x_i \exp\left(j \frac{2\pi}{N} ni\right) \quad (2.2)$$

At the transmitter, after the OFDM symbol generation using IDFT operation, the guard interval is added to the OFDM symbol. Then the signal is converted to analog and sent over the channel. At the receiver, after the analog to digital conversion, first the guard interval is removed and then demodulation is performed by a Discrete Fourier Transform (DFT) operation on the received OFDM symbol. In practice, the DFT functionality can be implemented using computationally efficient Fast Fourier Transforms (FFT) algorithms [14]. Nowadays, the advances in semiconductor technologies make large size and high speed FFT chips commercially affordable.

With perfect synchronization at the receiver, due to orthogonality of subcarriers, information on each subcarrier can be received without any interference from other subcarriers. For instance, if we consider (2.1) and the  $n$ -th subcarrier, in the receiver this subcarrier is demodulated using the Fourier transform as shown in (2.3).

Note that each subcarrier has exactly an integer number of cycles in the OFDM symbol duration  $T$ . So in (2.3) the integration of the exponential component over one  $T$  period, except for  $i = n$ , always results in zero since the frequency difference

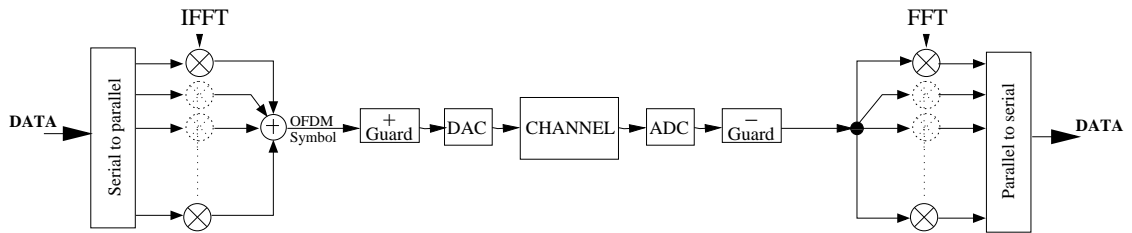


**Figure 2.3:** A simple OFDM transceiver [15].

of  $(i - n)/T$  always results in an integer number of cycles within the integration interval.

$$\begin{aligned}
 r &= \int_{t_s}^{t_s+T} \exp\left(-j2\pi\frac{n}{T}(t-t_s)\right) \sum_{i=-\frac{N}{2}}^{\frac{N}{2}-1} x_{i+\frac{N}{2}} \exp\left(j2\pi\frac{i}{T}(t-t_s)\right) dt \quad (2.3) \\
 &= \sum_{i=-\frac{N}{2}}^{\frac{N}{2}-1} x_{i+\frac{N}{2}} \int_{t_s}^{t_s+T} \exp\left(j2\pi\frac{i-n}{T}(t-t_s)\right) dt = x_{n+\frac{N}{2}}T
 \end{aligned}$$

A simple block diagram of the OFDM transceiver described above is depicted in Figure 2.3.

### 2.1.3 Cyclic prefix

As mentioned earlier, one of the advantages of OFDM is its robustness against multipath delay spread due to the relatively long OFDM symbol duration. In addition, to further reduce the ISI, a guard interval of length  $T_g$  is added at the beginning of each OFDM symbol. In order to preserve the subcarrier orthogonality and avoid ICI, the OFDM symbol is cyclically extended in the guard interval [11], i.e. the last  $N_g$  samples of the OFDM symbol is copied into the guard interval as shown in Figure 2.4. This guard interval is also known as *cyclic prefix*. Assuming a synchronized system, if the cyclic prefix length  $T_g$  is chosen, such that it is longer than the expected multipath delay spread, ISI and ICI can almost be completely avoided and the subcarrier orthogonality can be preserved.

Since the cyclic prefix provides no new information, it results in an overhead in time which reduces the system efficiency by a factor of  $N_g/(N + N_g)$ , where  $N_g$  is the number of cyclic prefix samples and  $N$  is the number of useful OFDM samples (i.e. the IFFT outputs). This overhead always exists, however, it is not significant if the number of useful OFDM samples is large (i.e. for a large number of subcarriers).

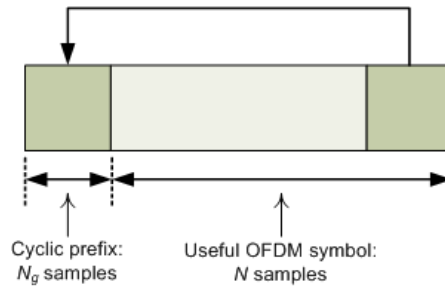


**Figure 2.4:** *Cyclic prefix.*

Moreover, the redundancy introduced by the cyclic prefix can be used for improving data estimation in the receiver [16] and also for synchronization purposes [17].

## 2.2 OFDMA

In a multi-user communication environment, the performance of the systems highly depends on the choice of the multiple access scheme. In recent years, a strong interest has been shown in Orthogonal Frequency Division Multiple Access (OFDMA) scheme, which, in fact, is a combination of OFDM and Frequency Division Multiple Access (FDMA). OFDMA was first proposed in [18] for cable TV (CATV) networks. Afterwards, an initial performance comparison of OFDMA with other access schemes e.g. OFDM-TDMA and OFDM-CDMA was done in [19] and [20] and it was shown that OFDMA outperforms the other schemes. Thus, it was adopted in the Interaction Channel for Digital Terrestrial Television (DVB-RCT) [21] and, more recently, it has been included in the 3GPP Long Term Evolution (LTE) and Mobile Worldwide Interoperability for Microwave Access (Mobile WiMAX, IEEE802.16e) standards [9, 10].

In an OFDMA system, several users transmit their data simultaneously over a disjoint set of subcarriers, often referred to as *subchannels*. Similar to OFDM, OFDMA has the ability to combat ISI and ICI resulting from the channel time dispersion. Moreover, the orthogonality of subcarriers prevents multiple access interference (MAI) among the users in the system. One of the important advantages of OFDMA is its ability to assign system resources (i.e. subcarriers and power) to different users based on their channel state information and exploit the frequency diversity and the so-called *multi-user* diversity [22]. Resource allocation in such system is discussed in more details in Section 2.3.

In spite of the great features, design and implementation of OFDMA systems have several challenges. One of the most prominent issues is the need for a very fine timing and frequency synchronization due to the fact that OFDMA, the same as OFDM, is extremely sensitive to timing errors and carrier frequency offsets [23, 24].

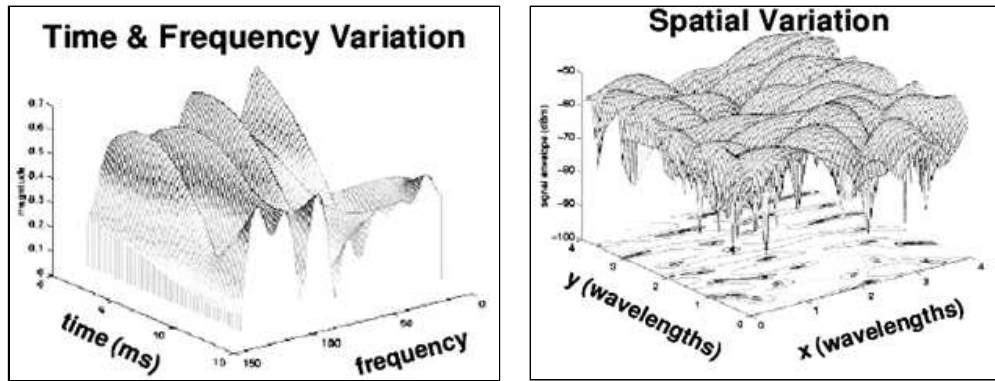


**Figure 2.5:** Channel variations in time, frequency and space.

This problem becomes more severe in the uplink of such systems where one OFDM symbol is generated by the contribution of many different users. Therefore, users must be perfectly aligned in time and frequency to maintain the orthogonality of subcarriers and prevent ICI and MAI. One usual method to protect the system against the possible misalignments, is using long guard intervals in OFDM symbols at the cost of its overhead and loss of the resources in time [25].

## 2.3 Resource allocation in OFDMA systems

Resource allocation in OFDMA systems refers to the allocation of subcarriers or subchannels (a groups of subcarriers) to different users as well as determining the power and modulation type per subcarrier. Due to the time- and frequency-selectivity of wireless channels, each subcarrier can experience different attenuation at different points in time and frequency, providing *frequency diversity*. Also in a multi-user environment, users are located at different places and a subcarrier's channel gain most probably differs from one user to another, providing *multi-user diversity*. Figure 2.5 shows the different channel variations. These variations in time, frequency and space can be exploited to assign the resources to users based on their channel state information (CSI).

### 2.3.1 Loading algorithms

One of the resources in an OFDMA systems that can be assigned based on the CSI is the amount of power per subcarrier. This can be accompanied by the modulation type per subcarrier. Such schemes are referred to as *dynamic power assignment* and *adaptive modulation* mechanisms. Considering a specific user at a certain point in time, different subcarriers have different attenuations in frequency, therefore, the scheduler can assign different amount of power to different subcarriers and based on

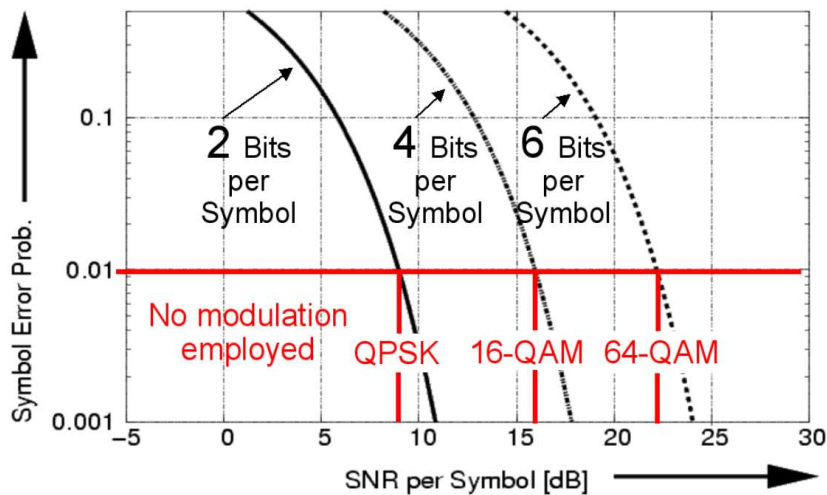


**Figure 2.6:** Symbol error probability vs. SNR for different QAM types (4-, 16-, 64-QAM).

the resulting Signal-to-Noise Ratios (SNR), it can also assign different modulation types to different subcarriers, in order to achieve a maximum system performance. The adaptive modulation is usually realized using a function ( $F_{snr2bit}$ ) which maps the SNR to one of the available modulation types. For instance, in Figure 2.6, the relationship between symbol error probability and SNR values for different types of QAM modulation is shown. If the target symbol error probability of the system is  $P_{err} = 10^{-2}$ , then the function  $F_{snr2bit}$  assigns 2 bits to subcarriers that their SNR values are between 8-16 dB, 4 bits to those with 16-22 dB SNR values and 6 bits to the subcarriers with SNR values more than 22 dB.

The above schemes are also known as *loading algorithms* and are based on the *water filling* theorem, known from information theory [26]. Hughes-Hartogs proposed the initial loading algorithm [27], and later on many algorithms have been proposed based on the Hughes-Hartogs algorithm to perform faster and achieve the optimal or sub-optimal resource allocation results [28–31].

There are two kinds of loading algorithms, *bit-loading* and *power-loading* algorithms. Bit-loading algorithms aim at maximizing the capacity by adopting the number of bits per subcarrier with respect to constraint on the available transmit power and the target bit error rate (BER), while power loading algorithms aim at minimizing the total transmit power by adopting the power level for each subcarrier with respect to constraint on the target data rate and BER. For more details on loading algorithms see [26] and [32].

### 2.3.2 Dynamic subcarrier assignments

In a multi-user environment, one of the other resources which can be assigned based on the CSI, except the power and modulation type, is the allocated subcarriers to different users. Considering a certain point in time, the attenuation of a subcarrier differs for different users (if they are separated with a minimum distance of one wavelength [33]), i.e. it can be in a deep fade for one user while having a low attenuation for another user. Assuming that the scheduler knows the instant CSI, it can periodically assign each subcarrier to the user which can use it best to achieve the system performance target (i.e. maximum capacity or minimum transmit power). This approach is called *dynamic subcarrier assignment*, also along with the loading algorithms, it is known as *dynamic OFDMA* [22, 34].

The above dynamic resource allocation schemes (subcarrier and power assignments) are based on the assumption that the scheduler knows (or has a good estimate of) the instant channel state information. More discussions on how to provide this information to the scheduler, i.e. using inband signaling or a separate control channel can be found in [35] and [36].

# Chapter 3

## Related Work and Thesis Approach

### 3.1 Related work on the OFDMA uplink

This section provide some of the related work on the OFDMA uplink. They are divided into two parts: related work on the synchronization methods including the studies on the use of frequency-domain guard bands, and related work on dynamic resource allocation in OFDMA systems.

#### 3.1.1 Synchronization techniques and guard bands

In the downlink of OFDMA systems, timing and frequency offsets are usually estimated by analyzing a pilot signal transmitted by the base station. Then, the synchronization can be accomplished using the similar methods as in single-user OFDM systems (since all the users receive the downlink data from the base station, with common timing and frequency errors [24]). However, this is not the case in the uplink, where the received signal at the base station is constructed out of transmitted signals from different users, each with different timing and frequency errors. The methods available for the downlink synchronization at the base station cannot be exactly applied to the uplink, since the correction of one user's offsets would misalign the others. Accordingly, in the uplink, each user must be separated from the others before starting the synchronization process [24]. Since this user separation is closely related to the subcarrier assignment method used in the system, different synchronization techniques for different assignment methods have been proposed in the literature. However, most of these methods assume a quasi-synchronous scenario [37], wherein, the length of the cyclic prefix is sufficiently long to compensate for the timing misalignments, and focus on the frequency estimation problem [25, 38, 39]. A comprehensive overview of the existing synchronization techniques for OFDMA systems is provided by Morelli et al. in [24].

Despite the numerous methods to combat timing and frequency offsets, there is always a chance for residual offsets among the users and the base station in a cellular OFDMA-based system, especially in the time domain. In [40], Wang et al. investigate the impact of residual offsets in the system and show that, even small residual offsets destroy the orthogonality among the OFDM subcarriers and, thus, lead to multiple access interference (MAI).

The use of frequency-domain guard bands to reduce the MAI due to synchronization errors in OFDMA systems, has first been studied by Tonello et al. in [41]. They present an analytical model for MAI (without any details on the derivation of the interference power in their model) and consider identical timing and frequency offsets for all users in a flat fading channel. They compare the signal-to-interference (SIR) and symbol error rate (SER) performance of the system in the static block-wise and interleaved subcarrier assignment methods and show that the block assignment scheme is more robust against MAI than the interleaved scheme. Their results also show that using guard bands in the block assignment scheme can improve the SIR and SER performance.

Later, Park et al., in [42], provide an analysis on the effects of timing misalignments in OFDMA uplink. They assume the timing misalignments to be i.i.d. for different users and uniformly distributed between zero and OFDM symbol duration. Their results show the SINR degradation for different values of maximum symbol timing misalignment and verify the SINR gain with guard subcarriers. In [43], You et al. study the effects of symbol timing misalignment in the system. In addition, they explore using different number of guard subcarriers in a block assignment scheme. Their results show a BER performance improvement as more guard subcarriers are used. However, they also show throughput degradation with the use of guard subcarriers.

In all of the above studies, the usage of guard bands has only been investigated with respect to SNR performance and in a static block assignment scheme. Thus, to the best of our knowledge, the incorporation of guard bands in the resource allocation optimization process has not been studied before.

### 3.1.2 Dynamic OFDMA systems

The work of Wong et al. in [22], is among the first and most cited papers which investigates the problem of dynamic resource allocation in the downlink of multi-user OFDM systems. They formulate an optimization problem, assuming perfect knowledge of the instantaneous channel gains for all users, to minimize the total transmit power subject to given transmission rate requirements. They show that this optimization problem is a combinatorial optimization problem and in order to make it tractable, they relax the integer constraint. Then, they prove that the new problem is a convex minimization problem, for which they derive the necessary

conditions for the optimal solution using the Lagrange technique. Moreover, they provide an iterative algorithm for calculating the Lagrangian multipliers. Since their optimal solution is based on the relaxation method, they introduce a sub-optimal multi-user adaptive OFDM (MAO) scheme and show that its performance is not far from the optimal continuous one. Despite the significant gain over fixed assignment schemes, their algorithm is difficult to implement and requires a large number of iterations to converge.

In [34], Rhee et al. formulate another optimization problem that maximizes the Shannon capacity for the worst user, based on the total power constraint in the downlink of a multi-user OFDM system. They also relax the integer constraint (allow for subchannel sharing among user) and convert the problem into a convex optimization problem. Then, they propose a sub-optimal algorithm with a low complexity to allocate the subchannels to users. It is shown that their sub-optimal algorithm performs almost as good as the optimal solution with a 2%–4% gap.

Later, Kim et al., in [44], convert the above originally non-linear optimal resource allocation problems, into linear ones and solve them by integer programming (IP). To reduce the complexity, they proposed a sub-optimal approach, which allocates the subcarriers based on the Linear Programming (LP) relaxation of the IP. Then, they use a greedy algorithm for bit loading. Their results show that the sub-optimal method produces almost the same results as the optimal one, with significant lower complexity.

Based on the optimization problem in [22], Kivanc et al., in [45], derive a computationally inexpensive method for subcarrier and power allocation in the downlink. Again, the objective is to minimize the total power consumption subject to a given minimum transmission rate requirement for each user. The allocation algorithm is divided into two steps. In the first step, the bandwidth assignment based on SNR (BABS) greedy algorithm uses the average SNR values to calculate the number of subcarriers that each user will get. In the next step, the specific assignment of subcarriers is done, for which they provide two different greedy algorithms. The first algorithm, Rate Craving Greedy (RCG), allocates each subcarrier to the user with the maximum transmission rate on that subcarrier. In the second algorithm, Amplitude Craving Greedy (ACG), the subcarrier is given to the user which has the highest gain on that subcarrier, given that the user has not exceeded the number of subcarriers calculated from the first step. Their proposed algorithms have comparable performance to the iterative one in [22], while being computationally cheap. More different approaches for dynamic resource allocation in OFDMA downlink can be found in [46–50].

Regarding the OFDMA uplink subcarrier and power allocation, in [51], Kim et al. formulate an sum-rate optimization problem based on the Shannon capacity formula for the Gaussian channel. The difference in their optimization problem with the usual downlink problems is that they consider each user has a specific power

constraint in the uplink. Moreover, the allocated power of one user to a subcarrier can differ from the allocated power of another user to the same subcarrier. Therefore, in their proposed optimization approach, power plays an important role. To solve the optimization problem, they relax the integer constraint on the assignment variable and prove that for the solution to be optimal, the assignment variable should have binary values. Therefore, the relaxation does not violate the intrinsic feature of OFDMA. Then, they propose a greedy algorithm for subcarrier allocation and an iterative water-filling power allocation algorithm. In the subcarrier allocation algorithm, first, the assigned power for all subcarrier/user pairs are calculated, either by using the water-filling algorithm or equal power distribution. Afterwards, each subcarrier is assigned to the user with the largest marginal rate. It is shown that their sub-optimal algorithms outperform the downlink algorithms. Their results also showed that the equal power distribution and water-filling algorithm in the uplink have similar performances.

In [52], Shen et al. investigate the design tradeoffs in the OFDMA uplink with respect to subcarrier assignment methods in different applications. They show that, for fixed and portable applications, where the propagation channels are almost static, the maximum throughput can be achieved when subcarriers are assigned to users with minimum frequency diversity, and for mobile services, the assignment method with maximum frequency diversity provides the maximum throughput.

All of the above dynamic resource allocation schemes, in the uplink (as well as the downlink) of OFDMA systems, assume a perfectly synchronized system and they do not take the multiple access interference into account. In this thesis, to the best of our knowledge, it is the first time that the use of frequency domain guard bands are incorporated in the dynamic resource allocation schemes to mitigate the possible MAI among users.

## 3.2 Thesis approach

As mentioned in Section 3.1.1, a common approach to mitigate MAI, is to use large time-domain guard intervals that assure orthogonality among subcarriers. As an alternative approach, in this thesis the usage of frequency-domain *guard bands* is explored to efficiently suppress MAI due to timing offsets. Using guard bands allows for short time-domain guard intervals, since guard bands can be added or omitted as needed, depending on the current subcarrier assignment situation. However, most approaches to optimize resource allocation in OFDMA uplink systems assume perfectly orthogonal subcarriers (see Section 3.1.2), and, thus, do not incorporate the MAI mitigation into the optimization problem. Since the MAI strongly depends on the distribution of subcarriers among the terminals, it needs to be considered in the dynamic subcarrier assignment mechanism.

In this thesis, the mitigation of MAI is incorporated into the subcarrier allocation process by using guard bands between frequencies assigned to individual users, which, allows for efficient resource usage. This way, we find the optimal trade off between the individuality in subcarrier assignments (which assures a high exploitation of multi-user and frequency diversity) and the number of necessary guard bands (that increases with the individuality of assignments) for the uplink.

The specific thesis goals can be summarized as follows:

- Study the impact of MAI and the effects of using frequency-domain guard bands on the SINR performance of the systems, to see whether employing guard bands can really protect against the MAI and improve the SINR. The results of this step should be inline with the previous works on this subject.
- Investigate the system capacity performance in the presence of MAI, as well as the impact of using guard bands on the system capacity. In this step, the trade off between using guard bands to mitigate MAI and having less subcarriers for data transmission will be studied.
- Finally, derive the optimization problem for the uplink and incorporate the guard bands into the dynamic subcarrier allocation mechanism. Study the capacity gains due to exploiting the diversity effects and using guard band for MAI mitigation.



# Chapter 4

## System Model

The system under consideration is a single cell  $c$  of a wireless cellular system consisting of a base station and user terminals. The cell has a radius of  $r_{\text{cell}}$ .  $N_u$  users are distributed among the cell following a uniform distribution. Each user is moving at a speed of  $v$ . Time is divided into frames of duration  $T_f$  which is also split into downlink and uplink phases. As we are interested in uplink transmission only, the downlink transmission phase is not considered any further.

### 4.1 Wireless channel

Each transmitted signal is affected by multipath fading channels and the additive white Gaussian noise (AWGN) with zero mean and variance  $\sigma^2$ . The uplink wireless channel for each user is modeled as a Rayleigh fading channel with exponential power delay profile [53].  $N_p$  fading paths are assumed. The individual path gains are independent with zero mean each. The  $p$ -th channel tap of  $k$ -th subcarrier of the  $u$ -th user is denoted by  $h_{k,u}^p$ . It is also assumed that the uplink channel response for each user varies independently from all other channels.

### 4.2 Transmitter

The considered system uses OFDM as its transmission scheme for uplink data transmission. Figure 4.1 shows the baseband block diagram of an OFDMA transmitter for uplink of the user  $u$ . It has a total uplink bandwidth of  $B_{\text{UL}}$  at center frequency  $f_c$ . The given bandwidth is split into  $N$  subcarriers (with a spacing of  $B_{\text{UL}}/N$  and a symbol length of  $T_s$  each). During a single frame, uplink data multiplexing is done by FDMA, where the smallest addressable bandwidth-unit

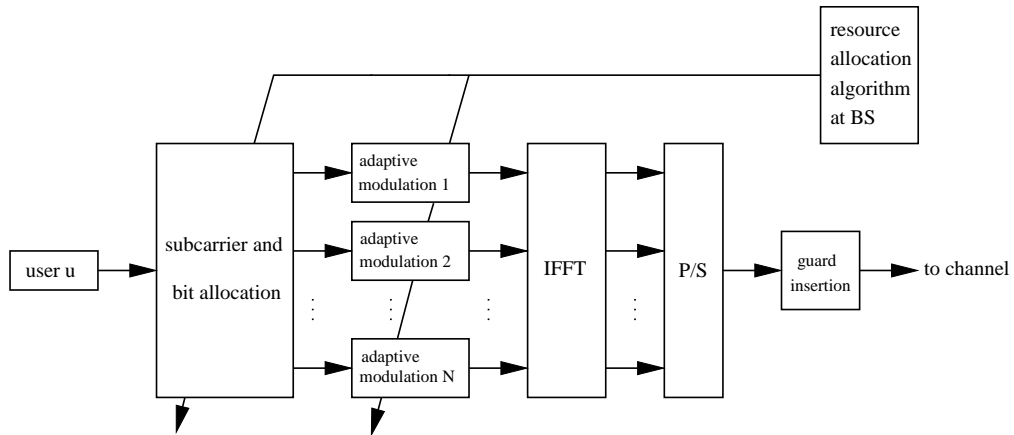


**Figure 4.1:** Block diagram of an OFDMA transmitter for uplink of the user  $u$ .

is a *subchannel*. In the frequency domain, a subchannel consists of a well defined number of adjacent subcarriers. In the time domain, a subchannel spans over all OFDM symbols available for user uplink data transmission of the respective frame.

In each frame, the base station allocates a certain set of subchannels with a certain amount of power for each subchannel to the users. The result of these allocations is then sent back to each user through a separate reliable control channel [36]. Three cases of user/subchannel assignments are considered: static block assignment (Figure 4.2(a)), static interleaved assignment (Figure 4.2(b)) and dynamic assignment. In the dynamic case, the assignment selection is based on the available CSI and the predicted interference situation per frame. It is also assumed that the maximum transmission power  $P_{\max}$  per cell is statically distributed over the subcarriers (i.e.  $P_T = P_{\max}/N$ ).

For the  $u$ -th user, the  $n$ -th subcarrier data symbol  $\{d_{n,u}\}$  is mapped to the symbol  $\{X_{n,u}\}$  as:

$$X_{n,u} = \begin{cases} d_{n,u}, & n \in \Gamma_u \\ 0, & n \notin \Gamma_u \end{cases} \quad (4.1)$$

where  $\Gamma_u$  is the set of subcarriers assigned to user  $u$ . These sets satisfy the condition in (4.2) which means users are assigned disjoint set of subcarrier.

$$\bigcup_{u=0}^{N_u-1} \Gamma_u = \{0, 1, \dots, N-1\}$$

$$\Gamma_u \cap \Gamma_{u'} = \emptyset \quad \text{if } u \neq u'. \quad (4.2)$$

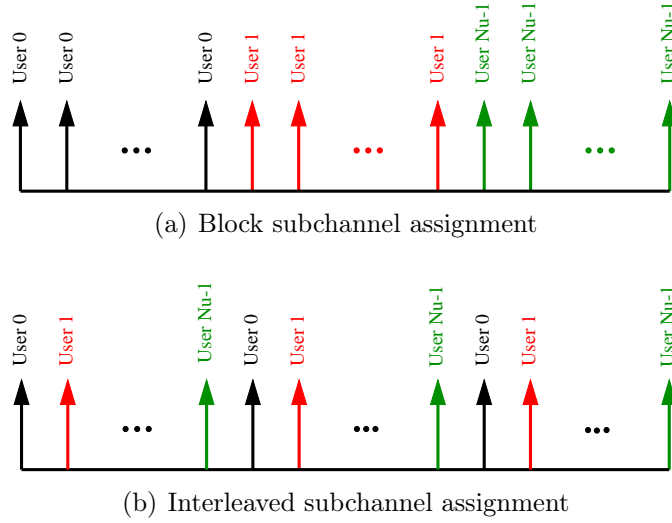


**Figure 4.2:** *Different subchannel assignment methods (assuming equal number of subchannels per user).*

According to the number of bits allocated to each subcarrier, adaptive modulation is performed [54], which chooses the appropriate modulation type for that subcarrier. This is then followed by the inverse fast Fourier transform. The IFFT output of the  $k$ -th subcarrier for the  $u$ -th user, according to (2.2), can be written as:

$$x_{k,u} = \sum_{n \in \Gamma_u} X_{n,u} e^{j \frac{2\pi n}{N} k} \quad 0 < k < N - 1, \quad (4.3)$$

where  $N$  is the number of subcarriers.

Afterwards the parallel data streams are converted to serial ones and prior to the transmission of the OFDM symbol, a cyclic prefix of length  $N_g = v_1 + v_2$  samples is added as a guard interval which results in total symbol duration of  $T = T_s + T_g$  in time domain. The distinction between  $v_1$  and  $v_2$  is made by imagining that  $v_1$  counteracts the time misalignments of the terminals while  $v_2$  counteracts the delayed echoes of the multipath channel.

### 4.3 Receiver

In the receiver, a bank of single user detectors is assumed as depicted in Figure 4.3. It is assumed that there is no carrier frequency offset between the transmitter and the receiver of all users. Upon arrival of the received signal from the channel,

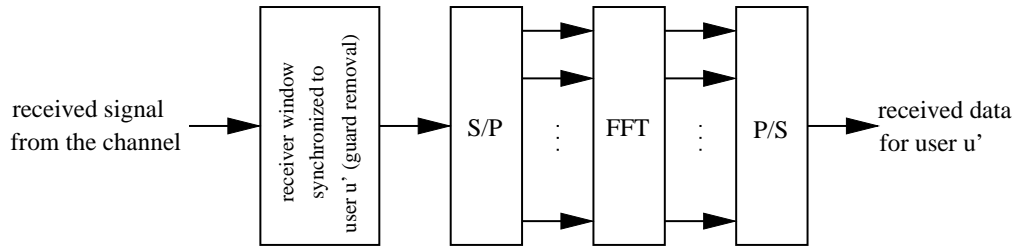


**Figure 4.3:** Block diagram of an OFDMA receiver for uplink of the user  $u'$ .

the receiver window, which is synchronized to the  $u'$ -th user, extracts a block of  $N$  samples starting from the middle of the guard interval  $N_g$  as follows:

$$\begin{array}{c}
 \overbrace{\hspace{15em}}^{N+N_g \text{ samples}} \\
 x_{N-v_2-v_1,u} \cdots \left[ x_{N-\frac{v_1}{2},u} \cdots x_{N-1,u} \quad x_{0,u} \cdots x_{N-\frac{v_1}{2}-1,u} \right] \cdots x_{N-1,u} \quad (4.4) \\
 \underbrace{\hspace{15em}}_{N \text{ samples}}
 \end{array}$$

However, users are not perfectly synchronized in the uplink and there is a symbol timing misalignment between users which is assumed to be normalized to the sample timing interval [42], i.e. the  $u$ -th user has a timing misalignment relative to  $u'$ -th user which corresponds to  $l_u$  samples.

Next, the block of  $N$  samples is converted to parallel and processed by the FFT during the duration  $T_s$ . Finally the data symbols of the  $u'$ -th user are reconstructed by converting the parallel FFT outputs to serial ones.

Now considering the transmitted symbols in (4.3) and the receiver window in (4.4), let  $x_{k,u,l_u}^p$  be the the  $k$ -th element of the  $N$ -point received window shifted by the symbol timing misalignment  $l_u$  on the channel tap  $p$ , then the  $k$ -th sample of the received signal at the input of the FFT can be written as:

$$y_k = \sum_{u=0}^{N_u-1} \sum_{p=0}^{N_p-1} h_{k,u}^p x_{k,u,l_u}^p + \omega_k \quad 0 < k < N - 1, \quad (4.5)$$

where  $\omega_k$  is the noise contribution.

And the FFT output for the  $u'$ -th user's  $n$ -th subcarrier is given by:

$$\begin{aligned}
Y_{n,u'} &= \frac{1}{N} \sum_{k=0}^{N-1} y_k e^{-j\frac{2\pi}{N}nk} & n \in \Gamma_{u'} \\
&= \frac{1}{N} \sum_{k=0}^{N-1} \sum_{u=0}^{N_u-1} \sum_{p=0}^{N_p-1} h_{k,u}^p x_{k,u,l_u}^p e^{-j\frac{2\pi}{N}nk} + W_{n,u'} & n \in \Gamma_{u'} \\
&= D_{n,u'} + I_{n,u'} + W_{n,u'} & n \in \Gamma_{u'}. \quad (4.6)
\end{aligned}$$

Consequently, the output signal consists of the desired signal  $D_{n,u'}$ , the multiple access interference (MAI) term  $I_{n,u'}$ , and the AWGN noise contribution  $W_{n,u'}$ .

From (4.3) and (4.6), the term  $D_{n,u'}$  can be written as:

$$D_{n,u'} = X_{n,u'} H_{n,u'}, \quad (4.7)$$

where,

$$H_{n,u'} = \sum_{p=0}^{N_p-1} h_{n,u'}^p e^{-j\frac{2\pi}{N}np}. \quad (4.8)$$

The term  $I_{n,u'}$  is the sum of the MAI from other users which is caused by the symbol timing misalignments. By substituting (4.3) in (4.6) and excluding the desired signal and noise, the MAI term can be written as:

$$I_{n,u'} = \sum_{u=0, u \neq u'}^{N_u-1} \tilde{X}_{n,u}, \quad (4.9)$$

where  $\tilde{X}_{n,u}$  is the contribution of the  $u$ -th user on subcarrier  $n$  which is given by:

$$\begin{aligned}
\tilde{X}_{n,u} &= \frac{1}{N} \sum_{k=0}^{N-1} \sum_{p=0}^{N_p-1} h_{k,u}^p x_{k,u,l_u}^p e^{-j\frac{2\pi}{N}nk} \\
&= \frac{1}{N} \sum_{k=0}^{N-1} \sum_{p=0}^{N_p-1} \sum_{m \in \Gamma_{u'}} h_{k,u}^p X_{m,u} e^{j\frac{2\pi}{N}(k-p+l_u)m} \cdot e^{-j\frac{2\pi}{N}nk}. \quad (4.10)
\end{aligned}$$

Finally the term  $W_{n,u'}$  in (4.6), which denotes the part of the output signal corresponding to the channel noise is,

$$W_{n,u'} = \frac{1}{N} \sum_{k=0}^{N-1} \omega_k e^{-j\frac{2\pi}{N}nk}. \quad (4.11)$$

## 4.4 Performance metrics

### 4.4.1 SINR

To evaluate the system performance and its degradation due to presence of the MAI, average signal-to-interference-plus-noise ratio (SINR) is calculated for each subcarrier at the output of the FFT. User  $u'$ -th's instant SINR value  $\gamma_{u',n}^{(t)}$  per subcarrier  $n$  ( $n \in \Gamma_{u'}$ ) varies over time due to its varying channel gain (reflecting path-loss, shadowing and fading) and MAI caused by surrounding users:

$$\gamma_{u',n}^{(t)} = \frac{P_{u',n}}{\sum_{u=0, u \neq u'}^{N_u-1} M_u^{(t)}(n|l_u) + \sigma^2}, \quad (4.12)$$

where

$$P_{u',n} = P_T \cdot \left( h_{u',n}^{(t)} \right)^2, \quad (4.13)$$

denotes the average received power on subcarrier  $n$  of user  $u'$ , and  $h_{u',n}^{(t)}$  denotes user  $u'$ -th's average channel gain on subcarrier  $n$  versus the base station.  $M_u^{(t)}(n|l_u)$  is the average power of the MAI generated on the  $n$ -th subcarrier by the  $u$ -th user conditioned on its time offset  $l_u$  relative to user  $u'$  (as described in the next section), and  $\sigma^2$  denotes the noise power per subcarrier.

### 4.4.2 User capacity

Average capacity per user is considered as another performance metric. It is defined as the amount of information bits that the user  $u$  can transmit over the wireless channel, using all the subcarriers assigned to it, averaged over all the uplink transmission phases. At each point in time, the number of bits that the  $u$ -th user

can transmit over its subcarrier  $n$ ,  $C_{u,n}^{(t)}$ , is a function of the perceived SINR on subcarrier  $n$  and the maximum admitted error rate  $P_{\text{err}}$  (see Section 2.3.1), i.e.,

$$C_{u,n}^{(t)} = F_{\text{sinr2bit}}(\gamma_{u,n}^{(t)}, P_{\text{err}}). \quad (4.14)$$

The user capacity as described above is the sum of all bits transmitted by a user, i.e.,

$$C_u^{(t)} = \sum_{n \in \Gamma_u} C_{u,n}^{(t)} \quad (4.15)$$

## 4.5 Multiple access interference

According to [40,41], the average power of the MAI generated on the  $n$ -th subcarrier by the  $u$ -th user conditioned on its relative time offset  $l_u$  is computed as (see the Section 4.5.1 for detailed mathematical analysis):

$$M_u^{(t)}(n|l_u) = \sum_{k \in \Gamma_u} \frac{P_{u,k}}{N^2} \frac{A_{n,k,l_u}^{(t)}}{\sin^2\left(\frac{\pi}{N}(n-k)\right)}. \quad (4.16)$$

The transmitted symbols are assumed i.i.d. with zero mean, thus, the MAI has zero mean, too. Recall that  $\Gamma_u$  is the set of subcarriers assigned to user  $u$ . The term  $A_{n,k,l_u}^{(t)}$  depends on the user's relative time offset  $l_u$  and the distance  $(n-k)$  in frequency between the desired subcarrier  $n$  and the interfering subcarrier  $k$ .

If the instant power per received path  $p$  is assumed to be computed as:

$$\Omega_{u,n,p}^{(t)} = E[|h_{u,n,p}^{(t)}|^2], \quad (4.17)$$

then, depending on user  $u$ -th's delay  $l_u$ ,  $A_{n,k,l_u}$  can be computed as [41]:

**Case I** For  $-N + \frac{v_1}{2} = a < l_u < b = -v_2 - \frac{v_1}{2}$ :

$$A_{n,k,l_u}^{(t)} = \sum_{p=0}^{N_p-1} \Omega_{u,k,p}^{(t)} \left[ \sin^2\left(\frac{\pi}{N}\left(p - l_u - \frac{v_1}{2} - v_2\right)(n - k)\right) + \sin^2\left(\frac{\pi}{N}\left(p - l_u - \frac{v_1}{2} - v_2 - N\right)(n - k)\right) \right],$$

**Case II** For  $-v_2 - \frac{v_1}{2} = b < l_u < c = N_p - 1 - v_2 - \frac{v_1}{2}$ :

$$A_{n,k,l_u}^{(t)} = \sum_{p=-b-|l_u|+1}^{N_p-1} \Omega_{u,k,p}^{(t)} \left[ \sin^2\left(\frac{\pi}{N}\left(p - l_u - \frac{v_1}{2} - v_2\right)(n - k)\right) + \sin^2\left(\frac{\pi}{N}\left(p - l_u - \frac{v_1}{2} - v_2 - N\right)(n - k)\right) \right],$$

**Case III** For  $N_p - 1 - v_2 - \frac{v_1}{2} = c < l_u < d = \frac{v_1}{2}$ :

$$A_{n,k,l_u}^{(t)} = 0$$

**Case IV** For  $\frac{v_1}{2} = d < l_u < e = N_p - 1 + \frac{v_1}{2}$ :

$$A_{n,k,l_u}^{(t)} = \sum_{p=0}^{|l_u|-\frac{v_1}{2}} \Omega_{u,k,p}^{(t)} \left[ \sin^2\left(\frac{\pi}{N}\left(p - l_u + \frac{v_1}{2}\right)(n - k)\right) + \sin^2\left(\frac{\pi}{N}\left(p - l_u + \frac{v_1}{2} + N\right)(n - k)\right) \right],$$

**Case V** For  $N_p - 1 + \frac{v_1}{2} = f < l_u < g = N + \frac{v_1}{2}$ :

$$A_{n,k,l_u}^{(t)} = \sum_{p=0}^{N_p-1} \Omega_{u,k,p}^{(t)} \left[ \sin^2\left(\frac{\pi}{N}\left(p - l_u + \frac{v_1}{2}\right)(n - k)\right) + \sin^2\left(\frac{\pi}{N}\left(p - l_u + \frac{v_1}{2} + N\right)(n - k)\right) \right].$$

### 4.5.1 MAI mathematical derivation

This section provides a detailed mathematical derivation of the multiple access interference and its power as shown in (4.16). For the sake of generality, it is assumed here that except the symbol timing misalignments between users, there is also a carrier frequency offset (CFO) between their local oscillators. In this case the received signal at the input to FFT in (4.5) is changed to:

$$y_k = \sum_{u=0}^{N_u-1} e^{-j\frac{2\pi}{N}k\Delta f_u} \sum_{p=0}^{N_p-1} h_{n,u}^p x_{k,u,l_u}^p + \omega_k \quad 0 < k < N - 1, \quad (4.18)$$

where  $\Delta f_u$  is the CFO of the  $u$ -th user relative to the  $u'$ -th user, normalized to the subcarrier spacing (i.e.  $\Delta f_u = (f_u - f_{u'})N/B_{UL}$ ).

Hence, the contribution of the  $u$ -th user to the MAI,  $\tilde{X}_{n,u}$  in (4.9), would be changed to:

$$\begin{aligned} \tilde{X}_{n,u} &= \frac{1}{N} \sum_{k=0}^{N-1} \sum_{p=0}^{N_p-1} h_{n,u}^p x_{k,u,l_u}^p e^{-j\frac{2\pi}{N}(n+\Delta f_u)k} \\ &= \frac{1}{N} \sum_{k=0}^{N-1} \sum_{p=0}^{N_p-1} \sum_{m \in \Gamma_{u'}} h_{n,u}^p X_{m,u} e^{j\frac{2\pi}{N}(k-p+l_u)m} \cdot e^{-j\frac{2\pi}{N}(n+\Delta f_u)k} \\ &= \frac{1}{N} \sum_{m \in \Gamma_{u'}} \sum_{p=0}^{N_p-1} h_{n,u}^p X_{m,u} e^{-j\frac{2\pi}{N}(p-l_u)m} \underbrace{\sum_{k=0}^{N-1} e^{-j\frac{2\pi}{N}(n-m+\Delta f_u)k}}_{\mathcal{J}_{m,i}^p}. \end{aligned} \quad (4.19)$$

In the previous equation, the symbol  $X_{m,u}$  is shifted by the total of  $(p - l_u)$  samples, where  $p$  is the delay samples due to the multipath environment and  $l_u$  is the delay samples due to relative timing offset of user  $u$  and  $u'$ . Now considering the receiver window in (4.4) for the  $u'$ -th user, different values of  $l_u$  lead to different results for the summation term  $\mathcal{J}_{m,i}^p$  in (4.19) and consequently different amount of interference from the  $u$ -th user  $\tilde{X}_{n,u}$ .

The MAI value based on the  $u$ -th user delay  $l_u$  and (4.4) can be categorized in different cases as follows:

**Case I** If the total delay,  $(p - l_u)$ , is such that the receiver window of  $u'$ -th user experiences interference from the *early* arriving symbols of  $u$ -th user, *for all the paths*, then we will have,

$$\begin{cases} \text{for } p = 0 : p - l_u > v_2 + \frac{v_1}{2} & \longrightarrow l_u < -v_2 - \frac{v_1}{2} \\ \text{for } p = 0 : p - l_u < N - \frac{v_1}{2} & \longrightarrow l_u > -N + \frac{v_1}{2} \end{cases}$$

$$\Rightarrow -N + \frac{v_1}{2} < l_u < -v_2 - \frac{v_1}{2}.$$

The first condition assures that the early symbols receiving in the first path are interfering with the  $u'$ -th user's receiver window. The second condition is to make sure that the delay  $l_u$  is such that the symbols in the last path are still in the receiver window, assuming  $N_p - 1 < v_2$ , i.e. the maximum delay spread is less than the guard period assigned to protect the multipath delay ( $v_2$ ).

In this case, the term  $\mathcal{J}_{m,i}^p$  in (4.19) will consist of two parts, early arriving symbols from the  $u$ -th user and the symbols from the  $u'$ -th user,

$$\mathcal{J}_{m,1}^p = \underbrace{\sum_{k=0}^{p-l_u-v_2-v_1/2-1} e^{-j\frac{2\pi}{N}(n-m+\Delta f_u)k}}_{\text{symbols of the } u\text{-th user}} + \underbrace{\sum_{k=p-l_u-v_2-v_1/2}^{N-1} e^{-j\frac{2\pi}{N}(n-m+\Delta f_u)k}}_{\text{symbols of the } u'\text{-th user}} \quad (4.20)$$

The above summations are two exponential series [55], which then result in

$$\begin{aligned} \mathcal{J}_{m,1}^p &= \frac{e^{-j\frac{2\pi}{N}(n-m+\Delta f_u)(p-l_u-v_2-v_1/2)} - 1}{e^{-j\frac{2\pi}{N}(n-m+\Delta f_u)} - 1} \\ &+ \frac{e^{j\frac{2\pi}{N}(n-m+\Delta f_u)(p-l_u-v_2-v_1/2-N)} - 1}{e^{-j\frac{2\pi}{N}(n-m+\Delta f_u)} - 1} \cdot e^{-j\frac{2\pi}{N}(n-m+\Delta f_u)(p-l_u-v_2-v_1/2)} \\ &= \frac{\sin \frac{\pi}{N}(n-m+\Delta f_u)(p-l_u-v_2-v_1/2)}{\sin \frac{\pi}{N}(n-m+\Delta f_u)} \cdot e^{-j\frac{\pi}{N}(n-m+\Delta f_u)(p-l_u-v_2-v_1/2-1)} \\ &- \frac{\sin \frac{\pi}{N}(n-m+\Delta f_u)(p-l_u-v_2-v_1/2-N)}{\sin \frac{\pi}{N}(n-m+\Delta f_u)} \cdot e^{-j\frac{\pi}{N}(n-m+\Delta f_u)(N+p-l_u-v_2-v_1/2-1)}. \end{aligned} \quad (4.21)$$

Since all the paths are treated the same in this case, the MAI from the  $u$ -th user can be achieved by simply substituting  $\mathcal{J}_{m,1}^p$  from (4.21) in (4.19):

$$\tilde{X}_{n,u} = \frac{1}{N} \sum_{m \in \Gamma_{u'}} \sum_{p=0}^{N_p^u-1} h_{n,u}^p X_{m,u} e^{-j \frac{2\pi}{N} (p-l_u)m} \cdot \mathcal{J}_{m,1}^p, \quad (4.22)$$

and if we assume that the transmitted data symbols on different subcarriers are independent of each other, with zero mean, then MAI has a zero mean, too. Let  $P_{m,u} = \mathbb{E} \{|X_{m,u}|^2\}$  be the received signal power of user  $u$  on subcarrier  $m$  and  $\Omega_{n,u}^p = \mathbb{E} \{|h_{n,u}^p|^2\}$  be the channel gain of subcarrier  $n$  of user  $u$  on path  $p$ .

With the above assumptions the power of MAI can be written as:

$$\begin{aligned} M_u(n|l_u) &= \mathbb{E} \left\{ |\tilde{X}_{n,u}|^2 \right\} \\ &= \frac{1}{N^2} \sum_{m \in \Gamma_{u'}} \sum_{p=0}^{N_p-1} \mathbb{E} \{|h_{n,u}^p|^2\} \cdot \mathbb{E} \{|X_{m,u}|^2\} \cdot \mathbb{E} \{|\mathcal{J}_{m,1}^p|^2\} \\ &= \frac{1}{N^2} \sum_{m \in \Gamma_{u'}} P_{m,u} \cdot \frac{A(n, k, \Delta f_u, l_u)}{\sin^2 \left( \frac{\pi}{N} (n - k + \Delta f_u) \right)}, \end{aligned} \quad (4.23)$$

where,

$$\begin{aligned} A(n, k, \Delta f_u, l_u) &= \sum_{p=0}^{N_p-1} \Omega_{n,u}^{(p)} \left[ \sin^2 \left( \frac{\pi}{N} (p - l_u - \frac{v_1}{2} - v_2)(n - k + \Delta f_u) \right) \right. \\ &\quad \left. + \sin^2 \left( \frac{\pi}{N} (p - l_u - \frac{v_1}{2} - v_2 - N)(n - k + \Delta f_u) \right) \right]. \end{aligned}$$

**Case II** If the total delay,  $(p - l_u)$ , is such that the receiver window of  $u'$ -th user experiences interference from the *early* arriving symbols of  $u$ -th user, *for some of the paths only*, then we will have,

$$\begin{cases} \text{for } p = 0 : & p - l_u < v_2 + \frac{v_1}{2} \quad \longrightarrow \quad l_u > -v_2 - \frac{v_1}{2} \\ \text{for } p = N_p - 1 : & p - l_u > v_2 + \frac{v_1}{2} \quad \longrightarrow \quad l_u < N_p - 1 - v_2 - \frac{v_1}{2} \end{cases}$$

$$\Rightarrow -v_2 - \frac{v_1}{2} < l_u < N_p - 1 - v_2 - \frac{v_1}{2}.$$

In this case, all the paths are not treated the same way since only some of them cause interference from  $u$ -th user. For the paths with no interference the term  $\mathcal{J}_m^p$  in (4.19) is:

$$\mathcal{J}_{m,2}^p = \sum_{k=0}^{N-1} e^{-j\frac{2\pi}{N}(n-m+\Delta f_u)k} = \frac{e^{-j2\pi(n-m+\Delta f_u)} - 1}{e^{-j\frac{2\pi}{N}(n-m+\Delta f_u)} - 1},$$

where  $n$  and  $m$  are subcarrier indexes, therefore  $(n - m)$  is an integer number and,

$$e^{j2\pi(n-m)} = \cos 2\pi(n-m) + j \sin 2\pi(n-m) = 1 + 0 \Rightarrow$$

$$\mathcal{J}_{m,2}^p = \frac{\sin(\pi\Delta f_u)}{\sin\frac{\pi}{N}(n-m+\Delta f_u)} \cdot e^{-j\pi\Delta f_u} e^{j\frac{\pi}{N}(n-m+\Delta f_u)}. \quad (4.24)$$

Considering different paths and using (4.21) and (4.24), the MAI from the  $u$ -th user can be written as:

$$\tilde{X}_{n,u} = \frac{1}{N} \sum_{m \in \Gamma_{u'}} X_{m,u} \left\{ \sum_{p=0}^{v_2+v_1/2-|l_u|} h_{n,u}^p e^{-j\frac{2\pi}{N}(p-l_u)m} \cdot \mathcal{J}_{m,2}^p \right.$$

$$\left. + \sum_{p=v_2+v_1/2-|l_u|+1}^{N_p-1} h_{n,u}^p e^{-j\frac{2\pi}{N}(p-l_u)m} \cdot \mathcal{J}_{m,1}^p \right\}, \quad (4.25)$$

and consequently the MAI power can be calculated from (4.23) with the term  $A(n, k, \Delta f_u, l_u)$  as:

$$\begin{aligned}
A(n, k, \Delta f_u, l_u) &= \sin^2(\pi \Delta f_u) \sum_{p=0}^{v_2+v_1/2-|l_u|} \Omega_{n,u}^p \\
&+ \sum_{p=v_2+v_1/2-|l_u|+1}^{N_p-1} \Omega_{n,u}^p \left[ \sin^2\left(\frac{\pi}{N}(p-l_u-\frac{v_1}{2}-v_2)(n-k+\Delta f_u)\right) \right. \\
&\left. + \sin^2\left(\frac{\pi}{N}(p-l_u-\frac{v_1}{2}-v_2-N)(n-k+\Delta f_u)\right) \right].
\end{aligned}$$

**Case III** If the total delay,  $(p-l_u)$ , is such that the receiver window of  $u'$ -th user experiences no interference from the early or late arriving symbols of  $u$ -th user, i.e. the total delay is not more than the guard interval, then we will have,

$$\begin{cases} \text{for } p=0: & p-l_u > -\frac{v_1}{2} & \longrightarrow l_u < \frac{v_1}{2} \\ \text{for } p=N_p-1: & p-l_u < v_2 + \frac{v_1}{2} & \longrightarrow l_u > N_p-1-v_2-\frac{v_1}{2} \end{cases}$$

$$\Rightarrow N_p-1-v_2-\frac{v_1}{2} < l_u < \frac{v_1}{2}.$$

In this case, again all the paths are treated the same and the MAI from the  $u$ -th user, by substituting (4.24) in (4.19) is:

$$\tilde{X}_{n,u} = \frac{1}{N} \sum_{m \in \Gamma_{u'}} \sum_{p=0}^{N_p-1} h_{n,u}^p X_{m,u} e^{-j \frac{2\pi}{N}(p-l_u)m} \cdot \mathcal{J}_{m,2}^p. \quad (4.26)$$

So, the MAI power from (4.23) can be calculated using,

$$A(n, k, \Delta f_u, l_u) = \sin^2(\pi \Delta f_u) \sum_{p=0}^{N_p-1} \Omega_{n,u}^p. \quad (4.27)$$

It can be seen that in this case, when the guard interval is large enough to counteract the timing delays, the MAI only results from the carrier frequency offsets.

**Case IV** If the total delay,  $(p - l_u)$ , is such that the receiver window of the  $u'$ -th user encounters interference from the *late* arriving symbols of  $u$ -th user, only for some of the paths, then we will have,

$$\begin{cases} \text{for } p = 0 : & p - l_u < -\frac{v_1}{2} \longrightarrow l_u > \frac{v_1}{2} \\ \text{for } p = N_p - 1 : & p - l_u > -\frac{v_1}{2} \longrightarrow l_u < N_p - 1 + \frac{v_1}{2} \end{cases}$$

$$\Rightarrow \frac{v_1}{2} < l_u < N_p - 1 + \frac{v_1}{2}$$

In this case, similar to Case II, paths are not treated the same since only some of them result in interference. So the term  $\mathcal{J}_m$  in (4.19) will be:

$$\begin{aligned} \mathcal{J}_{m,3}^p &= \underbrace{\sum_{k=0}^{p-l_u+N+v_1/2-1} e^{-j\frac{2\pi}{N}(n-m+\Delta f_u)k}}_{\text{symbols of the } u'\text{-th user}} + \underbrace{\sum_{k=p-l_u+N+v_1/2}^{N-1} e^{-j\frac{2\pi}{N}(n-m+\Delta f_u)k}}_{\text{symbols of the } u\text{-th user}} \\ &= \frac{e^{-j\frac{2\pi}{N}(n-m+\Delta f_u)(p-l_u+N+v_1/2)} - 1}{e^{-j\frac{2\pi}{N}(n-m+\Delta f_u)} - 1} \\ &\quad + \frac{e^{j\frac{2\pi}{N}(n-m+\Delta f_u)(p-l_u+v_1/2)} - 1}{e^{-j\frac{2\pi}{N}(n-m+\Delta f_u)} - 1} e^{-j\frac{2\pi}{N}(n-m+\Delta f_u)(p-l_u+N+v_1/2)} \\ &= \frac{\sin \frac{\pi}{N}(n-m+\Delta f_u)(p-l_u+N+v_1/2)}{\sin \frac{\pi}{N}(n-m+\Delta f_u)} e^{-j\frac{\pi}{N}(n-m+\Delta f_u)(p-l_u+N+v_1/2-1)} \\ &\quad - \frac{\sin \frac{\pi}{N}(n-m+\Delta f_u)(p-l_u+v_1/2)}{\sin \frac{\pi}{N}(n-m+\Delta f_u)} e^{-j\frac{\pi}{N}(n-m+\Delta f_u)(2N+v_1/2+p-l_u-1)}. \quad (4.28) \end{aligned}$$

Now considering different paths and using (4.24) and (4.28), the MAI term from the  $u$ -th user is:

$$\begin{aligned} \tilde{X}_{n,u} = & \frac{1}{N} \sum_{m \in \Gamma_{u'}} X_{m,u} \left\{ \sum_{p=0}^{|l_u|-v_1/2} h_{n,u}^p e^{-j \frac{2\pi}{N}(p-l_u)m} \cdot \mathcal{J}_{m,3}^p \right. \\ & \left. + \sum_{p=|l_u|-v_1/2+1}^{N_p-1} h_{n,u}^p e^{-j \frac{2\pi}{N}(p-l_u)m} \cdot \mathcal{J}_{m,2}^p \right\}, \end{aligned} \quad (4.29)$$

which results in the MAI power from (4.23) with:

$$\begin{aligned} A(n, k, \Delta f_u, l_u) = & \sum_{p=0}^{p=|l_u|-v_1/2} \Omega_{n,u}^p \left[ \sin^2\left(\frac{\pi}{N}(p-l_u + \frac{v_1}{2})(n-k + \Delta f_u)\right) \right. \\ & \left. + \sin^2\left(\frac{\pi}{N}(p-l_u + \frac{v_1}{2} + N)(n-k + \Delta f_u)\right) \right] \\ & + \sin^2(\pi \Delta f_u) \sum_{p=|l_u|-v_1/2+1}^{N_p-1} \Omega_{n,u}^p. \end{aligned}$$

**Case V** If the total delay is such high that for *all the paths*, the receiver window of  $u'$ -th user faces interference from the *late* arriving symbols of  $u$ -th user, then we will have,

$$\begin{cases} \text{for } p = N_p - 1 : & p - l_u < -\frac{v_1}{2} & \longrightarrow l_u > N_p - 1 + \frac{v_1}{2} \\ \text{for } p = 0 : & p - l_u > -N - \frac{v_1}{2} & \longrightarrow l_u < N + \frac{v_1}{2} \end{cases}$$

$$\Rightarrow N_p - 1 + \frac{v_1}{2} < l_u < N + \frac{v_1}{2}.$$

Since, similar to Case I, all the paths are treated the same in this case, by inserting  $\mathcal{J}_m$  from (4.28) in (4.19) the MAI term from  $u$ -th user can be written as:

$$\tilde{X}_{n,u} = \frac{1}{N} \sum_{m \in \Gamma_{u'}} \sum_{p=0}^{N_p-1} h_{n,u}^p X_{m,u} e^{-j \frac{2\pi}{N}(p-l_u)m} \cdot \mathcal{J}_{m,3}^p, \quad (4.30)$$

and the  $A(n, k, \Delta f_u, l_u)$  in (4.23) is:

$$\begin{aligned}
A(n, k, \Delta f_u, l_u) &= \sum_{p=0}^{N_p-1} \Omega_{n,u}^p \left[ \sin^2\left(\frac{\pi}{N}\left(p - l_u + \frac{v_1}{2}\right)(n - k + \Delta f_u)\right) \right. \\
&\quad \left. + \sin^2\left(\frac{\pi}{N}\left(p - l_u + \frac{v_1}{2} + N\right)(n - k + \Delta f_u)\right) \right].
\end{aligned}$$

Note that in all the above five cases, putting  $\Delta f_u = 0$  results in the MAI power as shown in (4.16). Investigating the effects of CFO is not in the scope of this thesis, however, in this section it is considered in the derivation of the MAI power to maintain the generality.

# Chapter 5

## The Use of Frequency Domain Guard Bands

In order to mitigate MAI due to users' timing misalignments in the uplink of an OFDMA system, a common approach is to use large cyclic prefixes per OFDM symbol as time-domain guard intervals [24, 56]. However, this approach not only comes with the expense of the extra overhead (due to having less time resources for data transmission per OFDM symbol), but also as soon as there are timing misalignments among users that are larger than the cyclic prefix, the system is again vulnerable to MAI. As mentioned earlier in Chapter 2, the length of the cyclic prefix is fixed and static in an OFDM-based system during the whole transmission time, and is the same for all users regardless of any possible changes in the systems during the transmission. Therefore, the selection of an appropriate cyclic prefix as guard interval has a significant impact on the system performance: choosing too large intervals limits the system capacity more than necessary, whereas choosing too short ones increases the probability of MAI, and thus, the error probability [41].

As an alternative to using long cyclic prefixes per OFDM symbol, frequency-domain *guard bands* can be used to separate frequency regions of users that experience different timing offsets versus the base station [41]. Using guard bands allows for short time-domain guard intervals, as guard bands can be added or omitted as needed, depending on the current subcarrier assignment situation.

### 5.1 Guard bands' impact on SINR performance

To investigate the effect of guard bands, let us consider a modification of a OFDMA-WiMAX system [9]. The modified system features short cyclic prefixes in combination with frequency-domain guard bands. Originally, a guard interval length of

$T_g = 11.4\mu s$  is suggested for the standard WiMAX uplink [57]. This number is quite large compared to the expected maximum delay spread (e.g.  $\Delta\tau_{ds} < 2\mu s$  in an microcell urban environment [58]). In the modified system approach, a guard interval length of  $T_g = 3\mu s$  is assumed. It is, thus, large enough to cope with the maximum delay spread, but does not protect against user timing misalignments. Hence, the overall OFDM symbol duration  $T$  in the modified system is shorter by the difference  $\Delta = 11.4\mu s - 3\mu s = 8.4\mu s$ . Accordingly, this difference is used to send more OFDM symbols per each uplink transmission phase. To integrate the guard bands into the existing WiMAX standard, a simple policy is considered: each user can use its allocated subchannels either as data subchannel or as guard band subchannel at the border of its frequency region.

Figure 5.1 shows the impact of MAI on the uplink SINR of subchannels (as defined in Section 4.4) assigned to one user in a WiMAX system with static block assignments for a sample configuration (10 users, 10 adjacent subchannels per user, described in Section 7.2 in detail). The *dot-dashed* curve belongs to an ideal system in which the users are perfectly synchronized and no MAI exists in the system. The *dashed* curve shows a more real system in which there are timing misalignments among users that result in MAI and performance degradation. This system uses a standard long cyclic prefix per OFDM symbol. The figure shows that, when MAI exists in the system, it is unlikely that even the long cyclic prefixes can eliminate it. Finally the *solid* curve shows the modified system in which short cyclic prefix is used per OFDM symbol. It can be seen that in this case, due to the smaller cyclic prefixes as guard intervals, the MAI has more impact on the performance than the case with long cyclic prefixes.

Figure 5.2 shows the impact of using frequency-domain guard bands featuring short cyclic prefixes (i.e. the *solid* curve). The *dashed* curve shows the effect of using one subchannel as a guard band at the beginning of each block of subchannels assigned to each user (e.g. subchannel 1 in the figure). It can be seen that using one subchannel as a guard band, decreases the MAI power on the other subchannels and thus, leads to SINR increase. The effect of using two guard subchannels is shown by the *dotted* curve. In this case the first and the last subchannels of each block is used as guards to protect against MAI. It shows that using two subchannels as guard bands mitigates the MAI even more and increases the SINR. Note that there is no SINR value for the guard subchannels since they are not modulated and no signal is transmitted in their frequency band.

If one compares the SINR of the remaining subchannels in this case, to the ideal case in Figure 5.1, it can be seen that in this example, MAI can completely be suppressed, if two subchannels per user are used as guards.

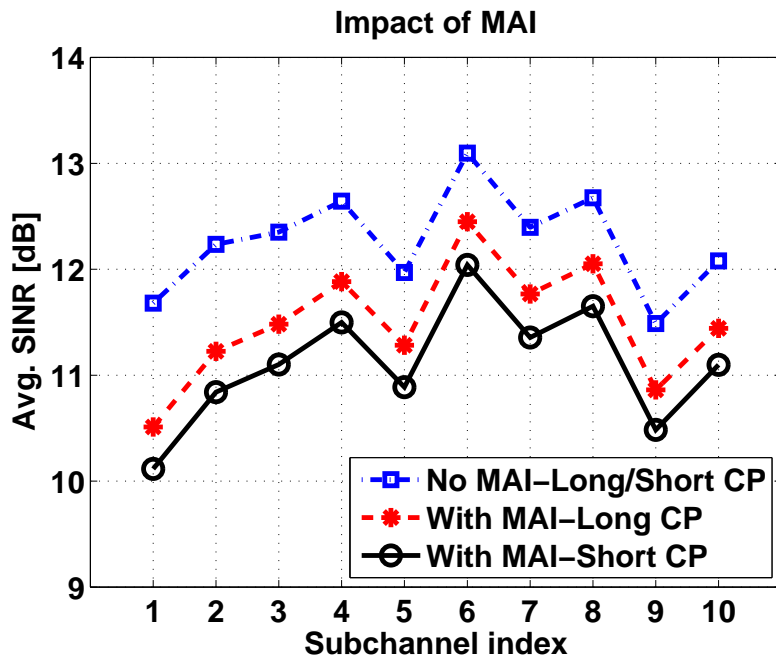


Figure 5.1: The impact of MAI on the average SINR per subchannel in the static block-wise assignment scenario for long and short cyclic prefixes (CP).

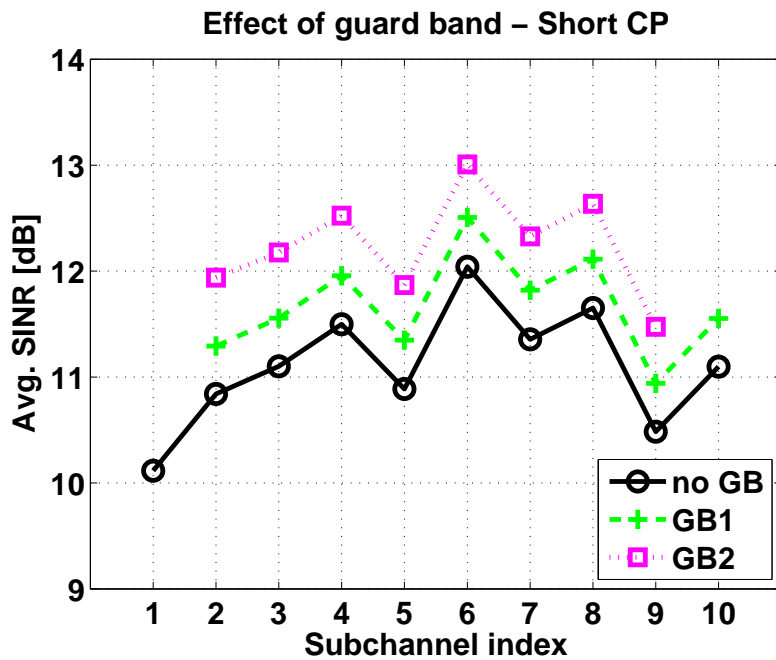


Figure 5.2: The impact of frequency-domain guard bands (GB) on SINR. In this example, MAI can completely be suppressed, if two subchannels per user are used as guards.

## 5.2 Guard bands' impact on capacity performance

In this section, the effect of using frequency-domain guard bands on per user and system capacity (as defined in Section 4.4) is investigated. For the system described in the previous section, the capacity comparison is shown between an ideal system (without MAI) and a real system, in which users are not perfectly synchronized in Table 5.1. Results for long and short guard intervals are shown. It can be seen that MAI considerably reduces the system capacity. However, even with MAI, the capacity is larger if short guard intervals are used. Apparently, the gain in capacity due to the transmission of additional OFDM symbols per frame is higher than the loss due to the increased MAI in this case.

**Table 5.1:** *Impact of MAI on system capacity in the static block assignments scenario [kbits/frame].*

<b>Long Guard Interval</b>	
Avg. cell capacity (no MAI)	66.86
Avg. cell capacity (w. MAI)	61.34
<b>Short Guard Interval</b>	
Avg. cell capacity (no MAI)	72.43
Avg. cell capacity (w. MAI)	65.20

Note that, there exists a trade off when using guard bands to mitigate the MAI: the higher the number of guard bands in use, the better the protection against MAI, but the lower the number of subchannels available for data transmission. Table 5.2 shows the average cell capacity, and Figure 5.3 shows the average per user capacity, for a system using no guard bands, one subchannel as a guard band (GB1) and two subchannel as a guard bands (GB2), featuring short cyclic prefixes and the block assignment method.

**Table 5.2:** *Impact of guard bands on the system capacity in the static block assignments scenario [kbits/frame].*

<b>Short Guard Interval</b>	
Avg. cell capacity (no GB)	65.20
Avg. cell capacity (GB1)	60.04
Avg. cell capacity (GB2)	54.47

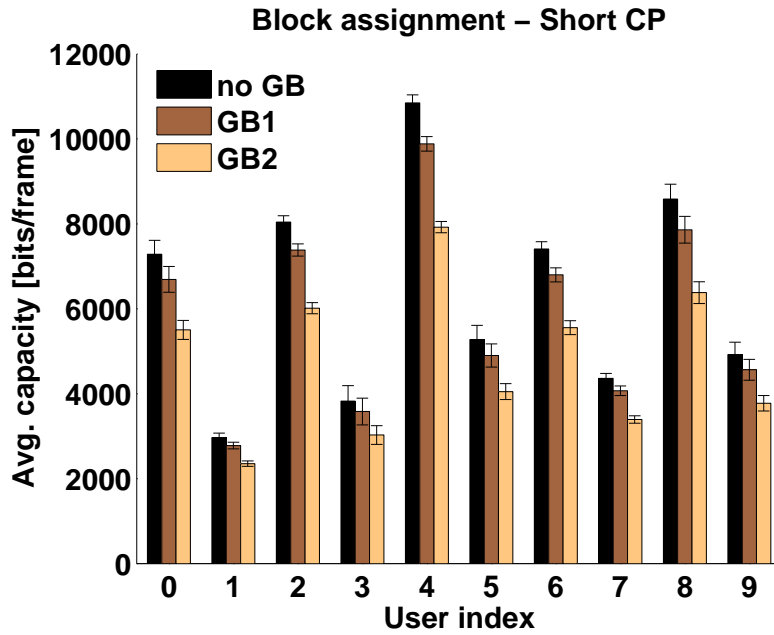


**Figure 5.3:** *The impact of guard bands on the average capacity per user in the static block-wise assignment scenario for a short cyclic prefix.*

It can be seen that in this simple and static case of guard band assignment, both the average user capacity and, consequently, the average cell capacity are decreased by using some of the subchannels as guard bands, instead of using them for data transmission. Therefore, there is a need for a more intelligent way to place the guards in order not to lose capacity when suppressing the MAI.



# Chapter 6

## Optimization Approaches

As it was shown in the previous chapter, using static guard bands in the block assignment method protects against the MAI at the cost of transmission efficiency. Therefore, the guard band placement strategy plays an important role in the throughput performance of the system and should be chosen more intelligently. In addition, it is well known that employing dynamic subchannel assignments in the downlink of an OFDMA system leads to a significant increase in the throughput performance compared to the completely static approaches, by taking advantage of frequency and multi-user diversity [22]. As described in Section 2.3.2, in the downlink of such systems, subchannels are assigned to users based on the instantaneous channel knowledge and the system optimization target (e.g. maximum system throughput or maximum per user throughput).

Hence, we would like to adopt the same mechanisms for the uplink of the system and include the guard band placement in the process of dynamic subchannel assignment to suppress MAI as well. Optimization problems for dynamic mechanisms in OFDMA systems are usually expressed as Integer Programs (IP) [44], which are a form of Linear Programs (LP), in which variables take on integer values only. More details on linear and integer programming can be found in [59].

In the following sections, initially an optimization model for the uplink is formulated and, afterwards, a sub-optimal approach is introduced, which is a modification of the downlink optimization problem. Along with a complementary algorithm, it yields a sub-optimal solution.

### 6.1 Optimization problem formulation

The system under consideration, employs dynamic subchannel assignment in combination with adaptive modulation and static power allocation (see Chapter 4). Each

subchannel  $n$  out of a set of  $N$  subchannels, is assigned to at most one terminal out of  $N_u$  terminals at a time, based on its instantaneous CSI and the predicted interference power on that subchannel (i.e. the subchannel's instant SINR). The set of all terminal-subchannel values for the instant SINR forms a  $N_u \times N$  matrix. The specific assignment of subchannel  $n$  to user terminal  $u$  at time  $t$  is the optimization variable. It is a binary variable  $x_{u,n}^{(t)}$ , which is set to one, if subchannel  $n$  is assigned to terminal  $u$ , and zero, otherwise:

$$x_{u,n}^{(t)} = \begin{cases} 1 & \text{if } n \text{ is assigned to } u \text{ at } t \\ 0 & \text{if } n \text{ is not assigned to } u \text{ at } t. \end{cases} \quad (6.1)$$

Depending on the instant SINR of each terminal-subchannel pair  $\gamma_{u,n}^{(t)}$ , and the target error rate  $P_{\text{err}}$ , one out of  $M$  available modulation types, is selected for each subchannel by the base station in each uplink transmission phase (adaptive modulation - see Section 4.4.2).

In the following, two optimization problems are explained and formulated: *raw-rate maximization* and *max-min capacity optimization*.

### 6.1.1 Raw-rate maximization

The first straightforward optimization approach, which can be applied to the system is to maximize the overall cell capacity (i.e. overall bit rate of the cell) in each uplink transmission phase. The formulation of this optimization problem is as follows:

$$\begin{aligned} \max \quad & \sum_{u,n} [F_{\text{sinr2bit}}(\gamma_{u,n}^{(t)}, P_{\text{err}}) \cdot x_{u,n}^{(t)}] \\ \text{s.t.} \quad & a) \sum_u x_{u,n}^{(t)} \leq 1 \quad \forall n, \end{aligned} \quad (6.2)$$

where  $F_{\text{sinr2bit}}(\gamma_{u,n}^{(t)}, P_{\text{err}})$  is the function that maps the perceived instant SINR to a certain modulation type. From (4.12) and (4.13), the instant SINR of terminal  $u$  on subchannel  $n$  at time  $t$  is:

$$\gamma_{u,n}^{(t)} = \frac{P_T \cdot \left(h_{u,n}^{(t)}\right)^2}{\sum_{u'=0, u' \neq u}^{N_u-1} M_{u'}^{(t)}(n|l_{u'}) \cdot x_{u,n}^{(t)} + \sigma^2}. \quad (6.3)$$

Constraint a) in Equation (6.2) assures that each subchannel is assigned to at most one user at a time. Since the sum is allowed to take values smaller than 1, i.e. 0 (since  $x_{u,n}^{(t)}$  is a *binary* optimization variable), a subchannel might not be assigned to any user and, thus, act as a guard band. A subchannel is selected to be a guard band, if the capacity gain due to the the suppression of MAI and the resulting improvement in SINR is larger than the capacity loss due to not transmitting data on that subchannel.

The raw-rate maximization might face the problem of fairness, as terminals with lower overall attenuations than others are favored in the subchannel assignment due to the optimization goal. As a consequence, some other terminals are hardly assigned subchannels for data transmission. Therefore, other optimization goals can be considered to address the fairness among terminals.

### 6.1.2 Max-min capacity optimization

Considering the fairness among users leads to an optimization approach, which maximizes the minimum user capacity (the weakest user's capacity) in the cell, while maximizing the overall cell capacity. This optimization problem is also known as *rate adaptive* in the literature [44], and can be formulated as:

$$\begin{aligned} \max \quad & \varepsilon + \omega \cdot \sum_{u,n} [F_{\text{sinr2bit}}(\gamma_{u,n}^{(t)}, P_{\text{err}}) \cdot x_{u,n}^{(t)}] \\ \text{s.t.} \quad & \text{a) } \sum_u x_{u,n}^{(t)} \leq 1 \quad \forall n \\ & \text{b) } \sum_n [F_{\text{sinr2bit}}(\gamma_{u,n}^{(t)}, P_{\text{err}}) \cdot x_{u,n}^{(t)}] \geq \varepsilon \quad \forall u, \end{aligned} \quad (6.4)$$

where  $\varepsilon$  is the lower bound for user capacity. Constraint a) has the same task as in the raw-rate maximization problem and guarantees the exclusive assignment of each subcarrier to one user. Constraint b) assures that the user capacity for all terminals is at least  $\varepsilon$ . The main optimization goal is to maximize this lower bound in each uplink transmission phase. The second term of the optimization

goal formulation assures that the overall cell capacity is maximized as an auxiliary goal, if different solutions for achieving the main goal exist. The scaling factor  $\omega$  ( $\omega \ll 1$ ), is chosen such that the auxiliary goal is targeted after the main goal is achieved.

Roughly speaking, this approach tries to distribute the subchannels in each uplink phase, in such a way that it reaches the highest possible minimum user capacity and, when at this limit, if still any subchannel is available, assigns it to the terminal with the lowest attenuation to yield a higher overall cell capacity.

In both of the above optimization approaches, the subchannel assignments are based on the instantaneous SINR values, and it can be seen from (6.3) that the instantaneous SINR depends on the MAI power, which itself is dependant on the subchannel distribution. In other words, since in the described approaches,  $\gamma_{u,n}^{(t)}$  in (6.3) is multiplied by  $x_{u,n}^{(t)}$ , this optimization problem is non-linear. It, thus, cannot be solved with linear program solvers, and is hard to handle. Therefore, a sub-optimal linear approach for guard band placement is developed and discussed in the next section.

## 6.2 Sub-optimal approaches

To overcome the issue of non-linearity of the previous optimization problems and make it possible to solve them with linear program solvers, (6.2) and (6.4) are modified as follows:

### Modified raw-rate maximization

$$\begin{aligned}
 \max \quad & \sum_{u,n} \left[ F_{\text{sinr2bit}}(\hat{\gamma}_{u,n}^{(t)}, P_{\text{err}}) \cdot x_{u,n,1}^{(t)} \right] \\
 \text{s.t.} \quad & a) \quad \sum_{u,m} x_{u,n,m}^{(t)} = 1 \quad \forall n \\
 & b) \quad \text{if } (x_{u,n,1}^{(t)} = 1 \quad \& \quad x_{u,n-1,1}^{(t)} = 0) \\
 & \quad \quad \quad \longrightarrow x_{u,n-1,0}^{(t)} = 1 \quad \forall u, n.
 \end{aligned} \tag{6.5}$$

### Modified max-min optimization

$$\begin{aligned}
 \max \quad & \varepsilon + \omega \cdot \sum_{u,n} \left[ F_{\text{sinr2bit}}(\hat{\gamma}_{u,n}^{(t)}, P_{\text{err}}) \cdot x_{u,n,1}^{(t)} \right] \\
 \text{s.t.} \quad & \text{a) } \sum_{u,m} x_{u,n,m}^{(t)} = 1 \quad \forall n \\
 & \text{b) } \sum_n \left[ F_{\text{sinr2bit}}(\hat{\gamma}_{u,n}^{(t)}, P_{\text{err}}) \cdot x_{u,n,1}^{(t)} \right] \geq \varepsilon \quad \forall u \\
 & \text{c) } \text{if } (x_{u,n,1}^{(t)} = 1 \quad \& \quad x_{u,n-1,1}^{(t)} = 0) \\
 & \quad \longrightarrow x_{u,n-1,0}^{(t)} = 1 \quad \forall u, n.
 \end{aligned} \tag{6.6}$$

Here, in both modified problems,  $\hat{\gamma}_{u,n}^{(t)}$  is the simple signal-to-noise ratio:

$$\hat{\gamma}_{u,n}^{(t)} = \frac{P_{u,n}}{\sigma^2}. \tag{6.7}$$

Hence, this optimization model is linear. The optimization variable  $x_{u,n,m}^{(t)}$  has three dimensions: the user terminal  $u$ , the subchannel  $n$ , as well as the mode of operation  $m$ . The latter is either set to 1 for data transmission or 0 for guard band operation. Since each subchannel is used either as guard band or for data transmission, the sum over all assignment variables per subchannel in constraint a) must be equal to 1. The last constraint assures that between any two subchannels assigned to different users there is at least one subchannel used as guard band.

The outcome of this approach is an optimal partitioning of the bandwidth among the users with respect to their instant SINR values, where the regions of any two users are separated by a guard band. However, since the MAI is not considered in the optimization problem, it is not optimal in terms of MAI suppression. Some of the selected guard bands might, thus, not be necessary and can be used for data transmission instead.

To figure out which of the assigned guard bands are really necessary and which ones are not, we performed some analysis on MAI power to study the frequency range that is affected by MAI around one subcarrier. Figure 6.1 shows the MAI power as a function of frequency distance around one subcarrier (no. 55), for different values of timing offset  $l_u$ , calculated from Equation (4.16). In this analysis, 100 subcarriers are assumed and the timing offset is normalized to the sampling time.

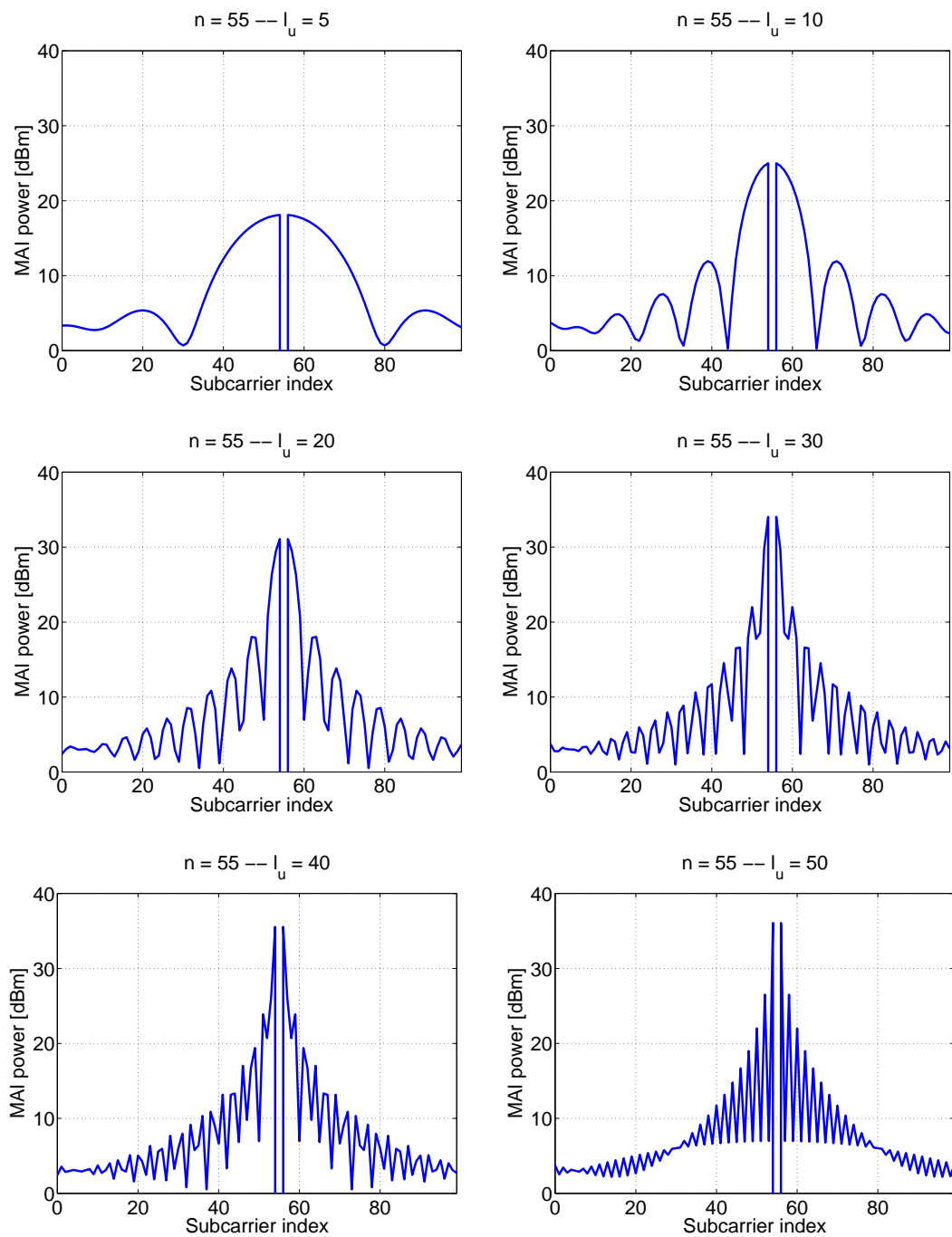


**Figure 6.1:** MAI power as a function of frequency distance for different values of timing offset.

Each graph of Figure 6.1 shows the impact of MAI on subcarrier 55 from the whole bandwidth. As expected, when distance in frequency to the desired subcarrier becomes larger, the MAI has less impact and vice versa.

Now if we want the MAI power on the desired subcarrier to be no more than e.g. 10 dBm, we can see that in all the graphs (i.e. for different values of  $l_u$ ), this threshold can be reached in a distance of about twenty subcarriers from the desired one. Also considering another MAI power threshold of 20 dBm, it can be seen that in the first graph, i.e. for  $l_u = 5$ , the MAI power is already less than the threshold value, and in all the other graphs, the threshold value can be achieved by moving about six or seven subcarriers away from the desired one. This implies that, to have the MAI power less than a certain threshold, e.g. 20 dBm, on a subcarrier, depending on the timing offsets, either no guard band is needed or a guard band width of around six subcarriers is required. In other words, to have the interference no more than a certain value, there might be two possible cases: the case in which, the timing offset is small, such that the resulting MAI is small enough and no guard band is required or the case in which, the timing offset is not small and, thus, there is a need to use guard bands. In the latter case, the guard band width, however, is fixed and does not differ for different values of timing offsets.

Using the above conclusions, we come up with an complementary algorithm, which is applied on the outcome of the optimization problem (6.5) or (6.6). This algorithm deselects the guard band between each two neighboring users which have no or a very small relative timing offset and assigns it for data transmission to the user that has a better SINR on that subchannel.

Algorithm 1,  $\Delta T_u$  is the  $u$ -th's user timing offset relative to the base station,  $\gamma_{u,n}^{(t)}$  is the SINR according to Equation (6.3), and  $\delta_{th}$  is the timing offset threshold that decides on the necessity of the guard band usage.

**Data:**  $\mathbf{X}_{\text{gb}}^{(t)}$ : Vector of GB subchannel indexes.

**Result:** Deselection of unnecessary guard bands and their assignments for data transmission.

```

1 for ( $n \in \mathbf{X}_{\text{gb}}^{(t)}$ ) do
2   find  $u$  and  $u'$  so that  $x_{u,n-1,1}^{(t)} = 1$  &  $x_{u',n+1,1}^{(t)} = 1$ 
3   if  $|\Delta T_u - \Delta T_{u'}| < \delta_{th}$  then
4     if  $\gamma_{u,n}^{(t)} > \gamma_{u',n}^{(t)}$  then
5        $x_{u,n,1}^{(t)} = 1$ 
6       else
7          $x_{u',n,1}^{(t)} = 1$ 
8       end
9     end
10  end
11 end

```

**Algorithm 1:** *Guard band deselection*

# Chapter 7

## Performance Evaluation

This chapter provides the the simulation results from the sub-optimal approaches. Moreover, the simulation methodology used in this thesis is explained and the different system and simulation parameters for the studied scenario are presented.

### 7.1 Methodology

To evaluate the approaches in Section 6.2, the system described in Chapter 4 is simulated using the free C++ discrete event simulation library OMNeT++ [60]. The instances per uplink phase of the optimization problems are passed to and solved by the LP solving software, ILOG CPLEX [61], using the ILOG Concert Technology. To assess the system performance metrics, i.e. average per user capacity and average cell capacity, 5 set of runs, each consists of 200 uplink phases, are simulated with different seeds for random number generators so as to get statistical confidence in the obtained results.

### 7.2 Simulation scenario

The following scenario is chosen for the simulations: one cell with the radius of  $r_{\text{cell}} = 500$  m, including a base station and 10 users are assumed. Users are uniformly distributed over the cell area and moving with a speed of 30 km/h according to [62]. The users' timing offsets, relative to the base station, are between 0 and the maximum of  $\Delta T_u = 25 \mu\text{s}$  (which is chosen to be about 25% of the OFDM symbol duration), with a uniform distribution. It is assumed that the timing misalignments are more due to the sampling clock drifts rather than the propagation delays, so they do not change during each simulation run.

The wireless channel is modeled according to the COST 231 model. The channel attenuation value reflects the three components of path loss, shadowing and fading. The path loss is modeled as:  $PL[dB] = 10 \log(K) - 10\alpha \log(d)$ , where  $10 \log(K) = -34.53$  dB and  $\alpha = 3.8$ , according to an urban microcell environment [58]. Shadowing is assumed to have a log-normal distribution with zero mean and standard deviation of  $\sigma_{sh} = 10$  dB. Fading is considered to follow the Rayleigh distribution with Jakes-like power spectrum. Maximum delay spread of  $1.8 \mu s$  and the noise power of  $\sigma^2 = -100$  dBm is considered.

The OFDMA system parameters are inline with the guidelines of the Mobile WiMAX standard employing OFDMA [9]. The carrier frequency of  $f_c = 2.5$  GHz is chosen. Channel bandwidth is 10 MHz which is divided into 100 subchannels. Every subchannel consists of 9 subcarriers with the size of 10.94 kHz each. The OFDM symbol duration without guard interval (cyclic prefix) is  $T_s = 91.5 \mu s$ . Originally the guard interval of length  $T_g = 11.4 \mu s$  is proposed for Mobile WiMAX [57], however in our approach we assume a shorter guard interval with duration of  $T_g = 3 \mu s$  which is long enough to counteract the effects of multipath delay spread but does not help for the MAI mitigation.

Adaptive modulation is applied on each subchannel. The target symbol error probability of  $P_{err} = 10^{-2}$  is chosen for the system.  $M = 4$  modulation types are available: BPSK, QPSK, 16-QAM and 64-QAM. Depending on the instantaneous SINR value, this scheme chooses the modulation type which results in the highest data rate with respect to the target error probability. Traffic is assumed to be full buffer, i.e. users always have data to transmit.

The summary of the system and simulation parameters is shown in Table 7.1.

## 7.3 Results

The simulation results are shown as the per user and cell capacity averaged over the whole 200 uplink phases and different simulation runs along with the 90% statistical confidence interval.

### 7.3.1 Raw-rate maximization

Table 7.2 shows the average cell capacity resulting from the raw-rate maximization with guard band (as described in Section 6.2), and without guard band, as well as the average cell capacity resulting from the static block assignment and interleaved assignment for comparison.

As it can be seen from the results, the static interleaved assignment method has

**Table 7.1:** *Simulation scenario, system and channel parameters.*

Parameters	Value
<b>Simulation Scenario</b>	
Cell Radius	500 m
Number of Mobile Stations (MS)	10
MS Maximum Speed	30 km/h
MS Maximum Timing Offset	25 $\mu$ s
Number of Simulated Uplink Phases	200
Number of Modulation Types	4 (1,2,4 or 6 bits/symbol)
Target Symbol Error Probability	$10^{-2}$
<b>System Parameters</b>	
Carrier Frequency	2.5 GHz
Channel Bandwidth	10 MHz
MS Maximum TX Power	23 dBm
Subcarrier Spacing	10.94 kHz
Subcarriers per Subchannel	9
Frame Duration	5 ms
OFDM Symbol Duration (without GI)	91.5 $\mu$ s
Guard Interval (GI) - long	11.4 $\mu$ s
Guard Interval (GI) - short	3.0 $\mu$ s
<b>Channel Parameters</b>	
Propagation Model	COST 231 Urban Microcell
Delay Spread	1.8 $\mu$ s
Path Loss Exponent	3.8
$10 \log(K)$	-34.53 dB
Penetration Loss	10 dB
Log-normal Shadowing SD	10 dB
Fading Model	Rayleigh
Noise Power	-100 dBm

the worst performance. The reason is that in this case each subchannel is adjacent to the subchannels from other users (see Figure 4.2(b)). Thus, the interference among them is the highest. The static block assignment method has a better protection against MAI compared to the interleaved method. This is due to the fact that subchannels, which are assigned to one user are perfectly orthogonal and do not interfere with each other. Thus, the amount of MAI in this scheme is inherently smaller, than in the interleaved approach and, consequently, the average cell capacity is larger.

Now, considering the raw-rate maximization approach which employs the guard bands to suppress the MAI, and also exploits the diversity effects of the wireless channel for subchannel assignment, we can see an increase in the overall cell capacity of about 29% compared to the static block assignment and about 44% compared to the interleaved assignment approach. Also it can be seen that using guard bands results in about 3% capacity gain in comparison with the case in which no guard band is used.

Figure 7.1 shows the average capacity of each user in this approach, with and without using guard bands. This figure exhibits the fairness issue of the raw-rate maximization problem, as discussed in Chapter 6. User 2 and User 4, are closer to the base station than others and have a lower overall attenuation, which leads them to be assigned most of the subchannels in each uplink transmission phase. On the other hand, User 1 is the weakest user of the cell and seldom assigned subchannel for its data transmission. It can also be observed in this figure, that the capacity of 60% of the users is improved by exploiting guard bands which causes the overall cell capacity to be also increased as shown in Table 7.2.

Therefore, these results indicate that the system can benefit from using guard bands as a means to combat the MAI and, thus, have a higher overall capacity.

### 7.3.2 Max-min optimization

To consider the fairness among users in the cell, the max-min optimization approach including guard bands is used (as described in Section 6.2). In this approach, the main optimization goal is to maximize the weakest user's capacity (i.e. User 1 in this scenario) and afterwards, when the lowest user capacity cannot be increased anymore, the auxiliary goal is to maximize the overall cell capacity. The scaling factor in Equation (6.6) is chosen to be  $\omega = 10^{-5}$ , so that the second part of the optimization problem does not impact the main goal.

Table 7.3(a) shows the comparison between the worst user capacity in static and dynamic subchannel assignment methods. It can be seen that the max-min approach with guard bands results in about 19% gain in the worst user capacity compared to the static block assignment and about 46% compared to the worst user in

**Table 7.2:** Average cell capacity in raw-rate maximization approach compared to static approaches [bits/frame].

Assignment	Cell Cap.	CI (90%)
Interleaved	56979	2040
Block (no GB)	63520	1588
Raw-rate (no GB)	79754	3776
Raw-rate (with GB)	81938	2868

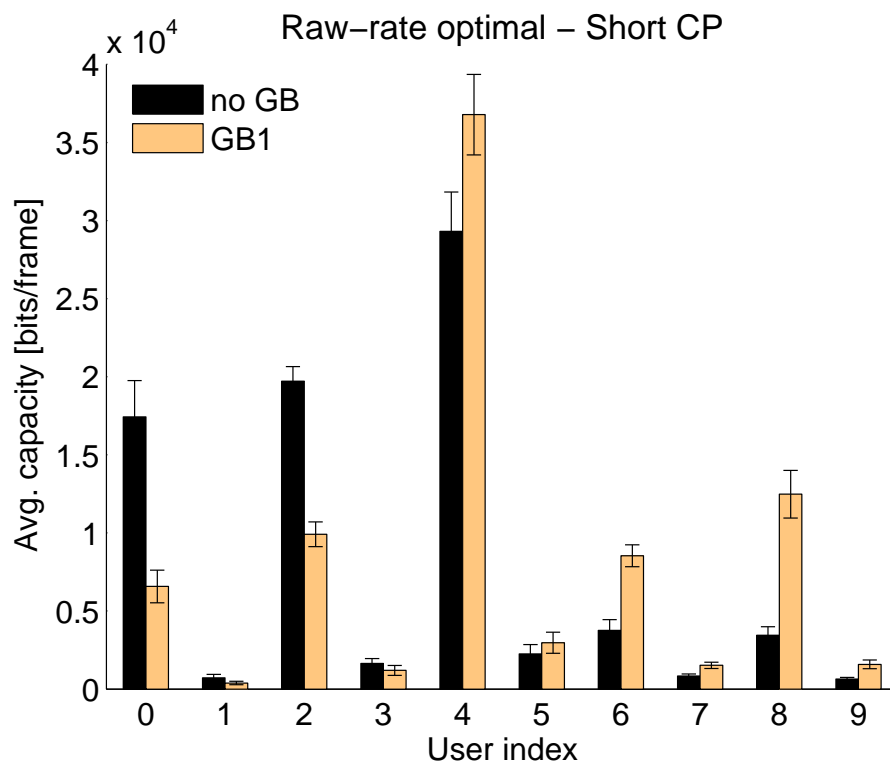


**Figure 7.1:** Average capacity per user in the raw-rate maximization approach, with and without guard bands. The large differences in users' capacities show the fairness issue in this approach, e.g. User 1 is hardly assigned any subchannel for data transmission.

**Table 7.3:** Capacity in max-min optimization approach: (a) primary and (b) auxiliary optimization goal [bits/frame].

(a) Average worst user capacity.

Assignment	Worst Cap.	CI (90%)
Interleaved	2413	472
Block (no GB)	2966	218
Max-min (no GB)	3427	558
Max-min (with GB)	3525	244

(b) Average cell capacity.

Assignment	Cell Cap.	CI (90%)
Interleaved	56979	2040
Block (no GB)	63520	1588
Max-min (no GB)	59804	2242
Max-min (with GB)	60228	3454

interleaved assignment. Also about 3% performance gain can be observed compared to the this approach without guard bands.

The performance comparison of this approach with respect to its auxiliary goal is shown in Table 7.3(b) where we can see that, as expected, adding the fairness condition reduces the overall cell capacity. In this scenario, the cell capacity is still 6% higher than the interleaved scheme, but about 5% less than the block assignment. However, recall that cell capacity is not the main target of this optimization approach.

The average capacity of each user in the block assignment and max-min approach with guard band is depicted in Figure 7.2. As can be seen in the figure, due to the fairness condition, the capacity per user is more evenly distributed among the users compared to the raw-rate maximization approach. Again, note that in this approach the primary objective is to maximize the worst user capacity in the cell, which in this scenario is User 1.

These results suggest that the system can also take advantages of guard bands to suppress the MAI and increase the minimum capacity in the cell.

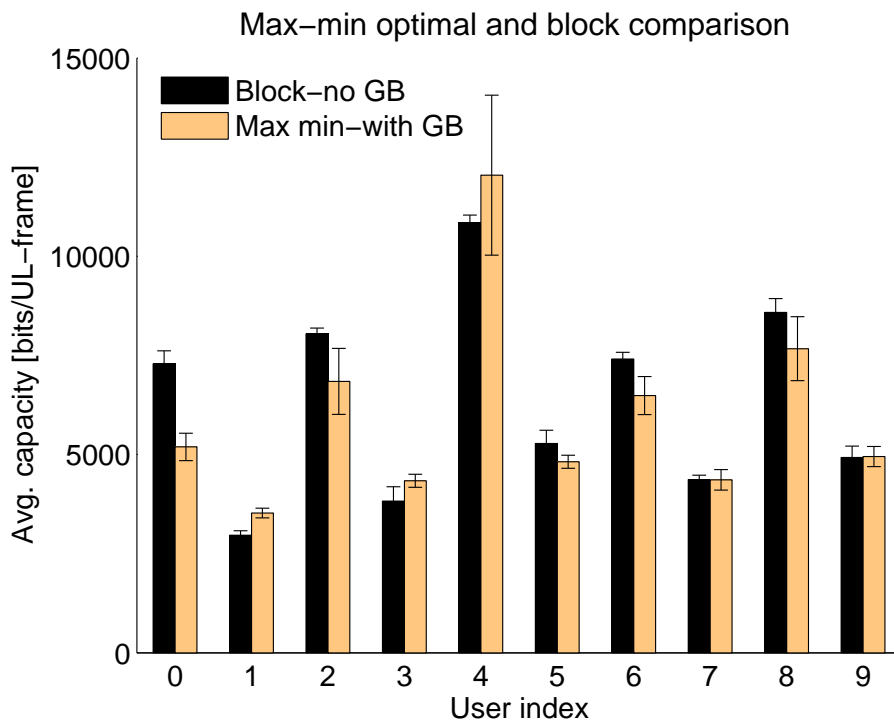


**Figure 7.2:** Average capacity per user in the max-min optimization approach with guard bands compared to the static block assignment. User 1's capacity is increased about 19% with this approach (main optimization objective).



# Chapter 8

## Conclusions

In this thesis, the use of frequency-domain guard bands as a means to counteract the effects of multiple access interference among users due to their timing misalignments, instead of using long cyclic prefixes as guard intervals in the uplink of an OFDMA system is investigated. The performance of this approach has been studied in a WiMAX-like system for two different subchannel assignment methods: namely, static block assignment and dynamic assignment.

The performance results from the static block assignment approach show that using some of the subchannels as guard bands between each two neighboring users, always improves the protection against MAI and leads to an increase in the SINR of the remaining subchannels. However, considering the overall cell capacity, using guard bands in this static method, does not result in a performance gain in terms of capacity. This is due to fact that the SINR gains are not large enough to compensate for having less resources, i.e. subchannels, available for data transmission.

In addition, the use of dynamic mechanisms for subchannel assignment, including guard band selection is studied. This approach can take advantage of diversity effects in the wireless channel assigning subchannels to different users. Therefore, guard bands can also be placed in a more dynamic fashion compared to the previous method. In this regard, two optimization approaches are considered: raw-rate maximization, which aims at maximizing the overall cell capacity, and max-min capacity optimization, which aims at maximizing the minimum user capacity as its primary objective and then, maximizing the cell capacity as its secondary objective. These two approaches are formulated and shown to be non-linear optimization problems, as a result of including the MAI in the optimization. Therefore, a linear program was developed for each of the optimization problems that in combination with one complementary algorithm yields a sub-optimal solution. Simulation results of the sub-optimal approaches show that, the system can benefit, in both cell capacity and the worst user capacity (based on the optimization goal), from using guard bands to reduce the impact of MAI.

The general conclusion which can be drawn from the given results is that the usage of frequency-domain guard bands is an efficient means to mitigate multiple access interference (MAI) in the uplink of OFDMA-based cellular systems. Using guard bands allows for shorter time-domain guard intervals and, thus, exposes additional time resources for data transmission in the system. Since the studied optimization approaches do not include the MAI power, the guard band placement strategy is still not optimal. However, it is shown that, even with a simple realization of the guard bands based on unused subchannels, an according system can gain in cell capacity and/or the minimum user capacity.

## 8.1 Future work

To accomplish more comprehensive performance evaluation of employing frequency-domain guard bands in the OFDMA uplink, the following future works are suggested:

- **More granular guard bands:** As demonstrated, already the usage of the simple subchannel-sized guard bands can provide valuable performance improvements, the first step for further research could address more fine-grained allocation of guard bands.
- **Heuristics:** As the well-known linear optimization problems used in the downlink of OFDMA-based systems are claimed to be NP-hard [32], integrating the guard band placement in those optimizations, makes them even more complex and leads to a significant computational overhead at the base station. Therefore, developing heuristic schemes, which yield an optimal or near-optimal solutions in a reasonable time, are of interest.
- **Bit-loading algorithms:** Dynamic power allocation schemes can also be included in the optimization approaches to evaluate the performance of a fully dynamic OFDMA system.

# Bibliography

- [1] I.F. Akyildiz, S. Mohanty, and Jiang Xie, “A ubiquitous mobile communication architecture for next-generation heterogeneous wireless systems,” *IEEE Communications Magazine*, vol. 43, no. 6, pp. S29–S36, June 2005.
- [2] ITU-R PDNR WP8F, *Vision, Framework and Overall Objectives of the Future Development of IMT-2000 and Systems beyond IMT-2000*, 2002.
- [3] J. Chuang and N. Sollenberger, “Beyond 3G: wideband wireless data access based on OFDM and dynamic packet assignment,” *IEEE Communications Magazine*, vol. 38, no. 7, pp. 78–87, July 2000.
- [4] S. Weinstein and P. Ebert, “Data transmission by frequency-division multiplexing using the discrete fourier transform,” *IEEE Transactions on Communications*, vol. 19, no. 5, pp. 628–634, October 1971.
- [5] P.S. Chow, J.C. Tu, and J.M. Cioffi, “Performance evaluation of a multichannel transceiver system for ADSL and VHDSL services,” *IEEE Journal on Selected Areas in Communications*, vol. 9, pp. 909–919, August 1991.
- [6] ETSI ETS 300 401 V1.3.3, *Radio broadcasting systems; Digital Audio Broadcasting (DAB) to mobile portable and fixed receivers*, May 2001.
- [7] ETSI EN 300 744 V1.5.1, *Digital Video Broadcasting (DVB); Framing structure, channel coding, and modulation for digital terrestrial television*, June 2004.
- [8] IEEE Std 802.11-2007, *IEEE Standard for Information Technology; Telecommunications and information exchange between systems; Local and metropolitan area network; Specific requirements; Part 11: Wireless LAN Medium Access Control (MAC) and Physical Layer (PHY) specifications*, June 2007.
- [9] IEEE Std 802.16e-2005, *IEEE Standard for local and metropolitan area networks Part 16: Air Interface for Fixed and Mobile Broadband Wireless Access Systems Amendment 2: Physical and Medium Access Control Layers for Combined Fixed and Mobile Operation in Licensed Bands and Corrigendum 1*, February 2006.

- 
- [10] 3GPP TR 25.814 V7.1.0, *3rd Generation Partnership Project; Technical Specification Group Radio Access Network; Physical layer aspects for evolved Universal Terrestrial Radio Access (UTRA)(Release 7)*, September 2006.
- [11] R. van Nee and R. Prasad, *OFDM for Wireless Multimedia Communications*, Artech House, Inc., 2000.
- [12] M. Bohge, J. Gross, M. Meyer, and A. Wolisz, "A new optimization model for dynamic power and sub-carrier allocations in packet-centric OFDMA cells," *Frequenz, Journal of RF-Engineering and Telecommunications, "Special Issue on Selected Papers of the 2006 International OFDM Workshop"*, vol. 61, no. 1-2, pp. 35–38, Jan./Feb. 2007.
- [13] Y. Wu and W.Y. Zou, "Orthogonal frequency division multiplexing: a multi-carrier modulation scheme," *IEEE Transactions on Consumer Electronics*, vol. 41, pp. 392–399, August 1995.
- [14] E. Bidet, D. Castelain, C. Joanblanq, and P. Senn, "A fast single-chip implementation of 8192 complex point FFT," *IEEE Journal of Solid-State Circuits*, vol. 30, pp. 300–305, 1995.
- [15] M. Bohge, "Bit loading versus dynamic sub-carrier assignment in multi-user OFDM-FDMA systems," June 2004, Diploma Thesis at Technical University of Berlin, Germany.
- [16] A. Tarighat and A.H. Sayed, "An optimum OFDM receiver exploiting cyclic prefix for improved data estimation," in *Proceedings of IEEE International Conference on Acoustics, Speech, and Signal Processing (ICASSP '03)*, 2003, vol. 4, pp. IV–217–220.
- [17] J.-J. van de Beek, P.O. Börjesson, M.-L. Boucheret, D. Landström, J.M. Arenas, P. Ödling, C. Ostberg, M. Wahlqvist, and S.K. Wilson, "A time and frequency synchronization scheme for multiuser OFDM," *IEEE Journal on Selected Areas in Communications*, vol. 17, no. 11, pp. 1900–1914, November 1999.
- [18] H. Sari, Y. Levy, and G. Karam, "Orthogonal frequency-division multiple access for the return channel on CATV networks," in *Proceedings International Conference on Telecommunications (ICT'96)*, April 1996, pp. 602–607.
- [19] H. Rohling and R. Gruneid, "Performance comparison of different multiple access schemes for the downlink of an OFDM communication system," in *IEEE 47th Vehicular Technology Conference*, May 1997, vol. 3, pp. 1365–1369.
- [20] H. Sari, Y. Levy, and G. Karam, "An analysis of orthogonal frequency-division multiple access," in *IEEE Global Telecommunications Conference (GLOBECOM '97)*, November 1997, vol. 3, pp. 1635–1639.

- [21] ETSI EN 301 958 DVB-RCT, *Digital Video Broadcasting (DVB); interaction channel for digital terrestrial television (DVB-RCT) incorporating multiple access OFDM*, March 2001.
- [22] C.Y. Wong, R.S. Cheng, K.B. Letaief, and R.D. Murch, "Multiuser OFDM with adaptive subcarrier, bit, and power allocation," *IEEE Journal on Selected Areas in Communications*, vol. 17, no. 10, pp. 1747–1758, October 1999.
- [23] T. Pollet, M. Van Bladel, and M. Moeneclaey, "BER sensitivity of OFDM systems to carrier frequency offset and Wiener phase noise," *IEEE Transactions on Communications*, vol. 43, no. 234, pp. 191–193, Feb./Mar./Apr. 1995.
- [24] M. Morelli, C.-C.J. Kuo, and M.-O Pun, "Synchronization techniques for orthogonal frequency division multiple access (OFDMA): A tutorial review," *Proceedings of IEEE*, vol. 97, no. 7, pp. 1394–1427, July 2007.
- [25] M.S. El-Tanany, Yiyang Wu, and L. Hazy, "OFDM uplink for interactive broadband wireless: analysis and simulation in the presence of carrier, clock and timing errors," *IEEE Transactions on Broadcasting*, vol. 47, no. 1, pp. 3–19, March 2001.
- [26] M. Bohge, J. Gross, M. Meyer, and A. Wolisz, "Dynamic resource allocation in ofdm systems: An overview of cross-layer optimization principles and techniques," *IEEE Network Magazine, Special Issue: "Evolution toward 4G wireless networking"*, vol. 21, no. 1, pp. 53–59, Jan./Feb. 2007.
- [27] D. Hughes-Hartogs, "Ensemble modem structure for imperfect transmission media," U.S. Patents Nos. 4,679,227 (July 1987), 4,731,816 (Mar. 1988), 4,833,706 (May 1988).
- [28] J.A.C. Bingham, "Multicarrier modulation for data transmission: an idea whose time has come," *IEEE Communications Magazine*, vol. 28, pp. 5–14, 1990.
- [29] P.S. Chow, J.M. Cioffi, and J.A.C. Bingham, "A practical discrete multitone transceiver loading algorithm for data transmission over spectrally shaped channels," *IEEE Transactions on Communications*, vol. 43, no. 234, pp. 773–775, February/March/April 1995.
- [30] J. Campello, "Practical bit loading for DMT," in *IEEE International Conference on Communications (ICC '99)*, 1999, vol. 2, pp. 801–805.
- [31] C.-H. Yih and E. Geraniotis, "Adaptive modulation, power allocation and control for ofdm wireless networks," in *Proceedings of the IEEE International Symposium on Personal, Indoor and Mobile Radio Communications, PIMRC 2000*, September 2000, vol. 2, pp. 809–813.

- 
- [32] J. Gross and M. Bohge, “Dynamic mechanisms in OFDM wireless systems: A survey on mathematical and system engineering contributions,” Tech. Rep. TKN-06-001, Telecommunication Networks Group, Technische Universität Berlin, May 2006.
- [33] D. Tse and P. Viswanath, *Fundamentals of Wireless Communication*, Cambridge University Press, 2005.
- [34] W. Rhee and J.M. Cioffi, “Increase in capacity of multiuser OFDM system using dynamic subchannel allocation,” in *Proceedings of IEEE Vehicular Technology Conference VTC*, May 2000, vol. 2, pp. 1085–1089.
- [35] J. Gross, H. Geerdes, H. Karl, and A. Wolisz, “Performance analysis of dynamic OFDMA systems with inband signaling,” *IEEE Journal on Selected Areas in Communications, Special Issue on 4G Wireless Systems*, vol. 24, no. 3, pp. 427–436, March 2006.
- [36] M. Bohge, A. Wolisz, A. Furuskar, and M. Lundevall, “Multi-user OFDM system performance subject to control channel reliability in a multi-cell environment,” in *Proceeding of the IEEE International Conference on Communications ICC’08*, pp. 3647–3652.
- [37] M.-O. Pun, M. Morelli, and C.-C.J. Kuo, “Maximum-likelihood synchronization and channel estimation for OFDMA uplink transmissions,” *IEEE Transactions on Communications*, vol. 54, no. 4, pp. 726–736, April 2006.
- [38] J. Choi, C. Lee, H.W. Jung, and Y.H. Lee, “Carrier frequency offset compensation for uplink of OFDM-FDMA systems,” *IEEE Communications Letters*, vol. 4, no. 12, pp. 414–416, December 2000.
- [39] Hwasun Yoo and Daesik Hong, “Edge sidelobe suppressor scheme for OFDMA uplink systems,” *IEEE Communications Letters*, vol. 7, no. 11, pp. 534–536, November 2003.
- [40] X. Wang, T.T. Tjhung, Y. Wu, and B. Caron, “SER performance evaluation and optimization of OFDM system with residual frequency and timing offsets from imperfect synchronization,” *IEEE Transactions on Broadcasting*, vol. 49, no. 2, pp. 170–177, June 2003.
- [41] A.M. Tonello, N. Laurenti, and S. Pupolin, “Analysis of the uplink of an asynchronous multi-user DMT OFDMA system impaired by time offsets, frequency offsets, and multi-path fading,” in *Proc. of IEEE Vehicular Technology Conference*, 2000, vol. 3, pp. 1094–1099.
- [42] M. Park, K. Ko, H. Yoo, and D. Hong, “Performance analysis of OFDMA uplink systems with symbol timing misalignment,” *IEEE Communications Letters*, vol. 7, no. 8, pp. 376–378, August 2003.

- [43] Y.-H. You, W.-G. Jeon, J.-W. Wee, S.-T. Kim, I. Hwang, and H.-K. Song, "OFDMA uplink performance for interactive wireless broadcasting," *IEEE Transactions on Broadcasting*, vol. 51, no. 3, pp. 383–388, September 2005.
- [44] I. Kim, H.L. Lee, B. Kim, and Y.H. Lee, "On the use of linear programming for dynamic subchannel and bit allocation in multiuser OFDM," in *Proceedings of IEEE Globecom 2001*, November 2001, vol. 6, pp. 3648–3652.
- [45] D. Kivanc, G. Li, and H. Lui, "Computationally efficient bandwidth allocation and power control for OFDMA," *IEEE Transactions on Wireless Communications*, vol. 2, no. 6, pp. 1150–1158, November 2003.
- [46] G. Song and Y. Li, "Cross-layer optimization for OFDM wireless networks – Part I," *IEEE Transactions on Wireless Communications*, vol. 4, no. 2, pp. 614–624, March 2005.
- [47] G. Song and Y. Li, "Cross-layer optimization for OFDM wireless networks – Part II," *IEEE Transactions on Wireless Communications*, vol. 4, no. 2, pp. 625–634, March 2005.
- [48] I.C. Wong, Zukang Shen, B.L. Evans, and J.G. Andrews, "A low complexity algorithm for proportional resource allocation in OFDMA systems," in *IEEE Workshop on Signal Processing Systems (SIPS)*, 2004, pp. 1–6.
- [49] Jiho Jang and Kwang Bok Lee, "Transmit power adaptation for multiuser OFDM systems," *IEEE Journal on Selected Areas in Communications*, vol. 21, pp. 171–178, 2003.
- [50] G. Munz, S. Pfletschinger, and J. Speidel, "An efficient waterfilling algorithm for multiple access OFDM," in *IEEE Global Telecommunications Conference (GLOBECOM '02)*, 2002, vol. 1, pp. 681–685.
- [51] Keunyoung Kim, Youngnam Han, and Seong-Lyun Kim, "Joint subcarrier and power allocation in uplink ofdma systems," *IEEE Communications Letters*, vol. 9, no. 6, pp. 526–528, June 2005.
- [52] Manyuan Shen, Guoqing Li, and Hui Liu, "Design tradeoffs in OFDMA traffic channels," in *Proceedings of IEEE International Conference on Acoustics, Speech, and Signal Processing (ICASSP '04)*, 2004, vol. 4, pp. iv–757–iv–760.
- [53] J.G. Proakis and M. Salehi, *Communication Systems Engineering*, Prentice-Hall, second edition, 2002.
- [54] T. Keller and L. Hanzo, "Adaptive multicarrier modulation: a convenient framework for time-frequency processing in wireless communications," *Proceedings of the IEEE*, vol. 88, no. 5, pp. 611–640, 2000.
- [55] Lennart Råde and Bertil Westergren, *Beta, Mathematics Handbook for Science and Engineering*, Studentlitteratur, fifth edition, 2004.

- [56] R. Nogueroles, M. Bossert, A. Donder, and V. Zyablov, “Performance of a random OFDMA system for mobile communications,” in *Proceedings of International Zurich Seminar on Broadband Communications*, February 1998, pp. 37–43.
- [57] WiMAX Forum, “Mobile WiMAX - Part II: A comparative analysis, v3.3,” 2006.
- [58] 3GPP Spatial Channel Model Ad-Hoc Group, “Spatial channel model text, SCM-132,” SCM Text V5.0, April 2003.
- [59] Optimization Technology Center of Northwestern University and Argonne National Laboratory, “Linear programming FAQ,” Posted at <http://www-unix.mcs.anl.gov/otc/Guide/faq/linear-programming-faq.html>, September 2005.
- [60] András Varga, *OMNeT++ User Manual 3.2*, March 2005.
- [61] *ILOG CPLEX 10.0 User's Manual*, January 2006.
- [62] Raj Jain, “WiMAX system-level evaluation methodology,” July 2006.